

012
013
014
015
016
017
018
019
020
021
022
023
024
025
026
027
028
029
030
031
032
033
034
035
036
037
038
039
040
041
042
043
044
045
046
047
048
049
050
051
052
053
054
055
056
057
058
059
060
061
062
063
064
065
066
067
068
069
070
071
072
073
074
075
076
077
078
079
080
081
082
083
084
085
086
087
088
089
090
091
092
093
094
095
096
097
098
099
100

The Interpretation of Electron Microscope Fractographs

C. D. BEACHEM

*Physical Metallurgy Branch
Metallurgy Division*

January 21, 1966



**U.S. NAVAL RESEARCH LABORATORY
Washington, D.C.**

DISTRIBUTION OF THIS DOCUMENT IS UNLIMITED.

000
001
002
003
004
005
006
007
008
009
010
011
012
013

CONTENTS

Abstract	1
Problem Status	1
Authorization	1
INTRODUCTION	1
FACTORS THAT AFFECT THE DENSITY OF FRACTOGRAPHS	1
Photography	2
Microscope	2
Replica	3
Artifacts	19
OTHER FACTORS OF INTERPRETATION	33
Stereo Viewing	33
Depth Measurements	33
Carbon Shadowing	35
Orienting Stereo Pairs	35
Precision Matching	39
Tailoring of Replicas	41
REPLICA FIDELITY	42
SUMMARY AND CONCLUDING REMARKS	43
REFERENCES	44
APPENDIX A—Figure for Practicing Unaided Stereo Viewing	47
APPENDIX B—Reprint of Fig. 40 to Permit Removal	49

For sale by the Superintendent of Documents, U.S. Government Printing Office
Washington, D.C., 20402 - Price 50 cents

012
011
010
009
008
007
006
005
004
003
002
001

The Interpretation of Electron Microscope Fractographs

C. D. BEACHEM

*Physical Metallurgy Branch
Metallurgy Division*

This report was prepared to aid the relative newcomer to electron fractography in the interpretation of fractographs. Accurate interpretation depends on understanding the effects of electron-microscope and replica variables on photographic densities in the fractographs. Briefly, some of these effects are as follows: Contrast decreases with increasing electron gun potential and lens aperture size. Electron density decreases and hence photographic density in the printed fractograph increases with the amount of replica material penetrated by the electrons. This, in turn, increases with an increase in the local thickness of the replica or with a decrease in the angle between the local replica surface and the incident electron beam. The thickness of the replica depends on the vacuum in the bell jar during formation of the replica, the angle of the local feature with respect to the depositing metal or carbon, and the distance between the feature and the source of the carbon or metal. During shadowing, convex features cast external shadows and tend to grow larger, while concave features contain their shadows and tend to remain the same size but to fill up with shadowing material. Interpretation is aided by stereoscopic viewing and by precision matching of mating fracture surfaces. Replica fidelity is a function of the choice of replication technique, with the direct carbon process generally being superior, and of the shape of both the features under study and immediately adjacent portions of the replicas.

This report can be only an aid to the newcomer, since nothing can adequately replace individual carefulness and experience. A fracture surface usually contains several species of features, and a few observations from one replica from one specimen are insufficient for most applications of fractography.

INTRODUCTION

A growing number of metallurgists and fracture mechanics investigators are beginning to study fracture surfaces at high magnifications using the electron microscope. Such studies require making replicas of the fracture surfaces and studying these in the microscope. The combination of high magnifications and the studying of replicas by transmission rather than of actual fracture surfaces by reflection makes interpretation difficult for the newcomer. Fracture surfaces appear different – sometimes startlingly so – and highly complex at electron microscope magnifications, especially to the newcomer.

To assure proper sampling of pertinent features on fracture surfaces, it is recommended that the person who is trying to obtain observations and data to complement his mechanical metallurgy or fracture mechanics data make his own replicas and examine them in the microscope himself. This requires a blending of portions of the dis-

ciplines of chemistry (replication, etching, *etc.*), electron microscopy, physical and mechanical metallurgy, and others depending upon the research objectives and techniques. The typical beginner has one or two of these backgrounds, but must learn something of the others before he can properly interpret fractographs.

The number of visitors who come to NRL for familiarization with interpretation of photographs taken of fine scale replica features (fractographs) prompted the preparation of this report.

The report deals mainly with the details of how one relates the black, white, and tones of gray of features on fractographs to the effects of replica and electron microscope variables and thus to the fracture surfaces themselves.

It is assumed that the reader already is familiar with photography, can make replicas, and can operate his electron microscope.

FACTORS THAT AFFECT THE DENSITY OF FRACTOGRAPHS

When one views a photograph of a replica taken in the electron microscope he sees only

NRL Problem M01-08; Projects RRMA 02-091/652-1/R007-01-01 and RR 007-06-46-5406. This concludes the phase of the problem dealing with the preparation of material to aid newcomers in the field of electron fractography. Work on research phases is continuing. Manuscript submitted October 5, 1965.

black, white, and shades of gray. His whole interpretation—and course of action to correct technique errors—depends upon his ability to recognize the things that produce the densities of specific portions of the fractograph.

In increasing order of usual significance, the main factors that influence density of the printed fractograph are (a) photography variables, (b) microscope variables, and (c) replica variables. By far the set of variables most important in interpretation are those involved in the preparation of replicas, since these must be understood and often controlled and varied in day-to-day operation. In brief the replica variables that a fracture analyst must recognize as affecting the density of a printed fractograph are: the basic technique (dry strip, direct, two stage, three stage), the replica material, the replica thickness, the angle of the replica with respect to the depositing shadowing material and carbon, the vacuum in the evaporator during deposition of the shadowing material and carbon, the introduction of artifacts during replication, and the angle of the replica with respect to the electron beam in the microscope. Microscope variables he must recognize are: the sizes of the apertures, the cathode-anode voltage (electron speed), the focus, the alignment, replica change in the microscope (from overheating, buildup of electrical charge, contamination), and stability. In more detail the following considerations must be made concerning the photography, microscope, and replica variables which the analyst must control or may find useful to vary.

Photography

Though most darkroom techniques become well standardized after a month or so of operation, the interpretation of electron fractographs can sometimes be facilitated by selection of specific conditions for individual fractographs. High contrast, for example, may be more appealing to the eye in a specific fractograph, while some of the fine detail used in interpretation may be best seen in low contrast.

Magnifications should be chosen to make the feature of interest occupy an appreciable portion of the field of view.

Reverse printing (emulsion side of the negative up in the enlarger) is often necessary in

the precision matching studies described later in the report.

Microscope

For the best interpretation, a person who uses fractography to study fracture should examine his own replicas in the microscope. Experience with operating the microscope enables one to recognize and correct microscope errors as well as to obtain a select fractograph with optimum exposure, contrast, angle, and magnification.

Condenser apertures should be small enough to prevent overheating the replica. One of the distinguishing features of an overheated replica is the balling up or reticulation of the shadowing material, as shown in Fig. 1. Other things that may happen in the microscope are the electrostatic charging of extracted particles with a resultant fuzzy image or the melting of particles, causing the local destruction of the replica.

The effect on contrast of changing the accelerating potential of the electron gun is shown in Fig. 2. It has been found that increasing this voltage decreases the contrast, and decreased contrast is useful where the replica is unusually thick. It is sometimes necessary to make replicas extra thick to make them mechanically stable, and these usually can be best viewed at 100 kV.

Fractograph crispness depends upon many factors. Focus, astigmatism, and beam alignment must be controlled to various degrees at various magnifications. The accuracy of focus and astigmatism correction required for high-resolution work at 100,000X are overly sufficient and not required at the magnifications of up to 5000 or 10,000X that apply to most fractography work.

Contamination of the replica (due partly to oil vapors depositing and baking onto the replica) while it is exposed to the electron beam is an important factor when extended viewing times are necessary. Replica contamination is illustrated in Fig. 3. These fractographs were taken at 40 kV and a beam current of 10 μ A; higher values of either would hasten the contamination.

Fields from alternating currents near the microscope column, dirty apertures, specimen holders, or specimen, or changes in lens current can move the image while the negative is being exposed. These are usually characterized by blurring in one direction (transverse or rotation).

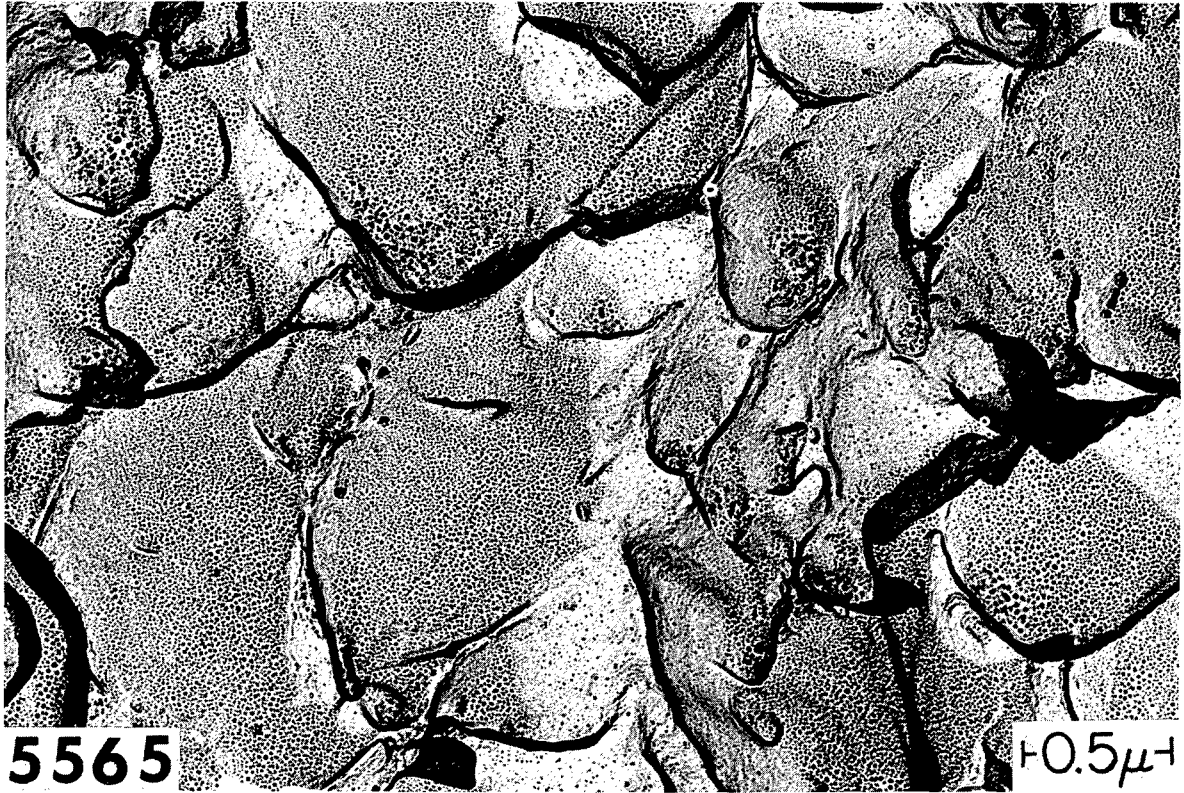


Fig. 1 — Example of a replica overheated in the electron beam, showing the grainy appearance of reticulated shadowing material (in this instance, palladium). This is a two-stage (cellulose acetate-carbon) replica of dimples in nickel. (Original magnification, 45,000X.)

Replica

The transmission microscope requires the electrons to pass through the object being studied, and since electrons can penetrate only a few hundred or a thousand angstroms, one cannot put a fractured piece of metal into it and study the fracture surface. Therefore one must put a replica of the fracture surface into the microscope for study.

These replicas may be prepared in numerous ways, but they are all extremely thin and are more fragile than the soot or dust that a shaft of sunlight makes visible drifting around in practically still air. Consequently, replicas have the following disadvantages:

1. They must be supported on a grid, which means that one cannot see the entire replica. Parts (sometimes more than half) are hidden by the opaque grid bars.

2. They are almost always prepared in such a manner that they are in contact with a liquid (acetone, alcohol, water, *etc.*) when they are most fragile. The surface tension of the liquid, as it evaporates, destroys some of the features of the replicas. Features larger than 20 microns stand a very good chance of collapsing or ripping when the liquid evaporates. Features that are 50 to 100 microns or larger are almost certain to be distorted or destroyed.

3. Since replicas are not the fracture surfaces themselves, their fidelity is limited. Details on the replicas smaller than about 40 to 50 angstroms or larger than about 50 microns are almost certain to be to an appreciable degree nonrepresentative of the fracture surface. This leaves about four orders of magnitude in which useful information can be obtained. However, within this range there are a number of artifact structures which must be recognized during interpretation.

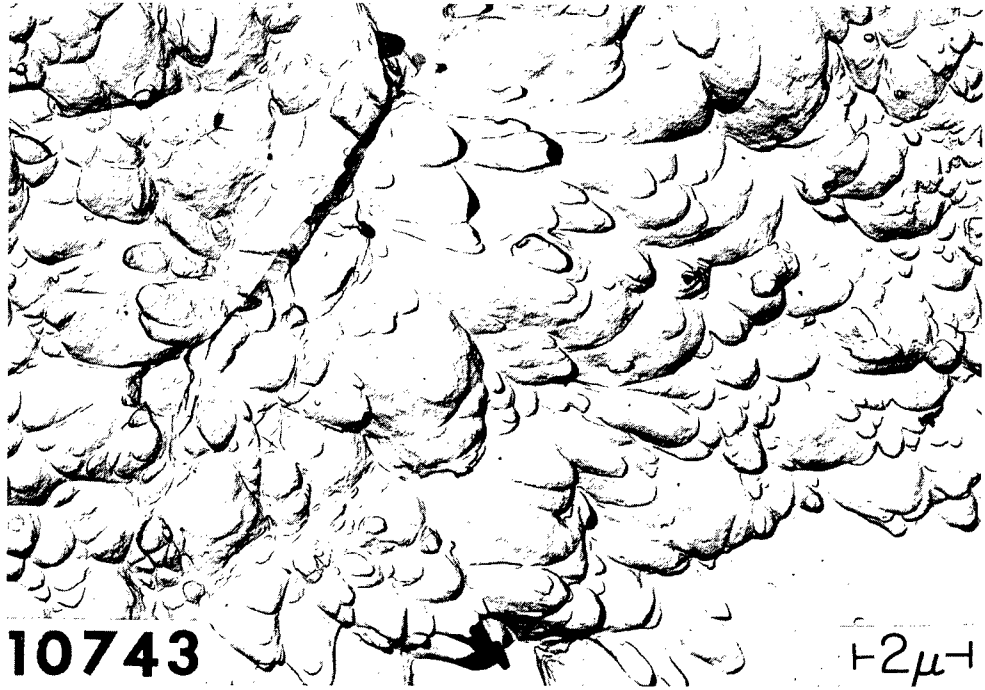


Fig. 2 - The effect of accelerating potential of the electron gun upon the contrast of the image. The top fractograph was taken at 40,000 volts and the bottom at 100,000 volts. This is a two-stage (cellulose acetate-carbon) replica of dimples in AISI 4340 steel. (Original magnification, 9000X.)

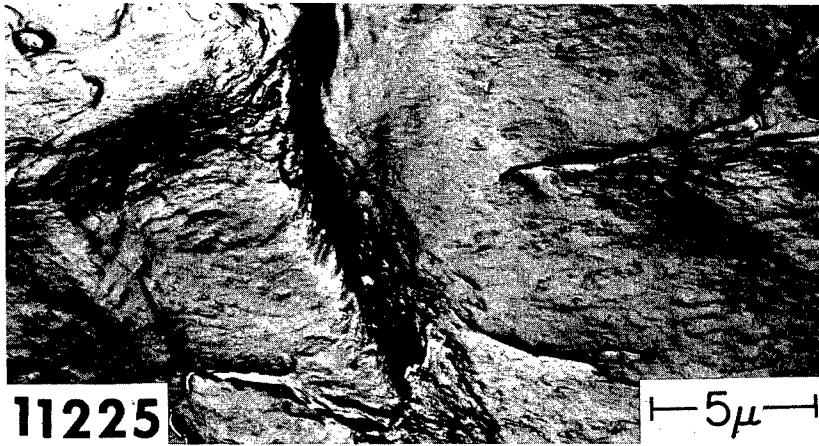
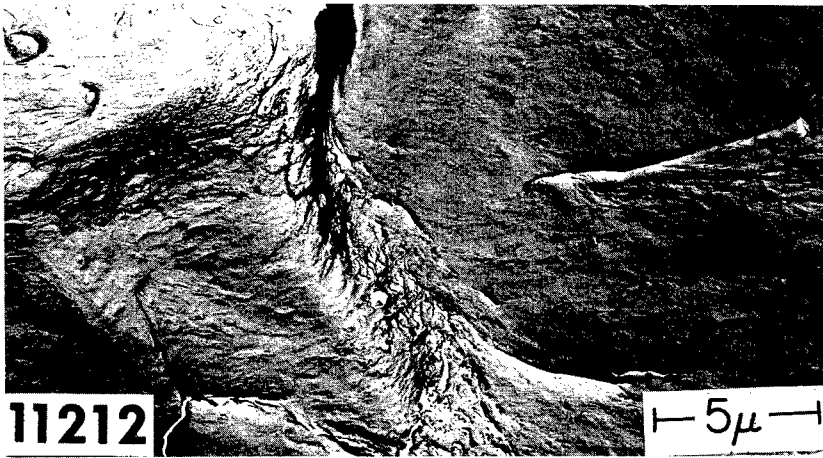


Fig. 3 – Contamination of a replica in the electron microscope. The replica was exposed to 40-kV electrons at a beam current of 10 μ A. Top, start of test. Center, after 3 hours. Bottom, after 8 hours. (Original magnification, 6000X.)

If the reader does not already know the rudiments of replication it may be wise for him to visit one or more laboratories where replicas are routinely made. References 1 through 4 also are recommended for those interested in learning techniques. Replica techniques will be referred to frequently in this report but only to the extent that they have a bearing on interpretation.

Figure 4 illustrates some replica variables which must be remembered in the interpretation of every fractograph. The density of the image (and of the printed fractograph) depends upon the degree to which the electrons are scattered when they pass through the replica. This scattering is due to: the scattering cross section of the elements in the replica (Ref. 1, page 246), as illustrated in row 1 of Fig. 4; the number of such atoms encountered by the electrons as they pass through the replica—which depends upon both the thickness of the replica and the angle at which the replica is oriented with respect to the incident beam of electrons in the microscope, as illustrated in rows 2 and 3; and the microscope electron gun electrical potential setting (Ref. 1, page 301).

The amount of replica material that the electrons pass through is dependent upon the relationship $T \sec \theta$ where T is the local replica

thickness and θ is the angle between the thickness direction of the replica and the direction of the incident electron beam. This means that if the limiting amount of material which the electrons can penetrate under given circumstances is 500\AA , and the replica is 50\AA thick, the angle which gives an opaque image is more than 84° (i.e., 6° from the replica being parallel to the electron beam). If, however, the electrons can penetrate 1000\AA and the replica is 200\AA thick, the angle for a locally opaque image is more than 78° . Thus the replica must be locally quite steeply tilted away from the plane of the grid in order to cause an opaque image due to its orientation. The effects of this orientation enter into the interpretation at lesser angles, however, and the effect of the angle often approaches or exceeds the effect of local replica thickness.

The density variations on the image are usually affected by all of the above factors. In other words, every feature of the fracture surface must be analyzed with these factors in mind. Various facets, dimples, steps, ridges, etc., of the fracture surface will be reproduced in the replica as a combination of thickness, materials, and orientation. Neighboring facets on a printed fractograph may have the same photographic density which results from different combinations of thickness, material, and orientation.

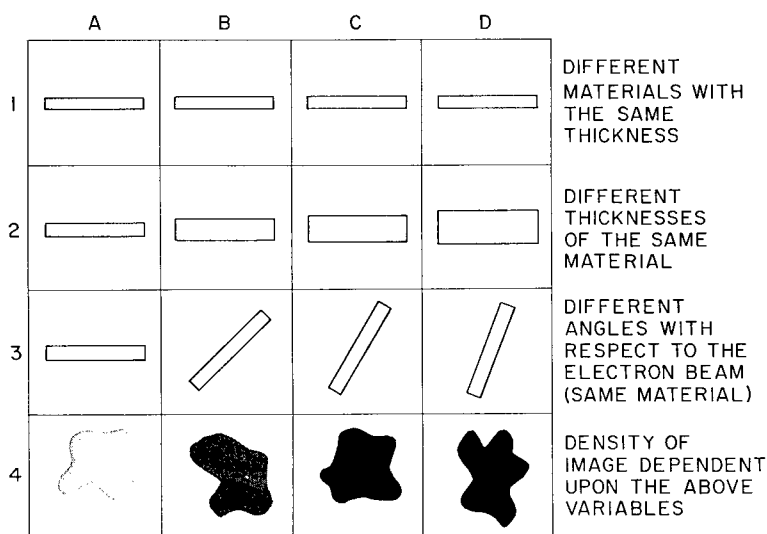


Fig. 4 — Three replica variables that play major roles in determining the density of the final image

The thickness of the evaporated film depends upon (a) the distance between the source and the substrate, (b) the evaporation rate of the evaporant, (c) the degree of vacuum in the bell jar, and (d) the angle of the substrate surface with respect to the depositing material. The first three of these become standardized in most laboratories after a short period of operation. The last is not often subject to control on a microscopic scale. One can orient the overall plane of the replica with respect to the depositing vapor, but the micron-sized features are ordinarily oriented at such varying angles that the local thickness of the deposited material varies considerably and is essentially uncontrolled.

Figure 5 is a simple illustration of the effect of incident (shadowing) angle upon the thickness of the deposited material. At A, where the angle is about 90° , the deposit is much thicker than at D, where the angle is about 20° . At E the film would have negligible thickness in comparison to the others. It should be noted, however, that, even at E, electrostatic attraction, van der Waal's forces, and scattering due to an incomplete vacuum will contribute to a deposit.

An example of the effect of shadowing angle upon image intensity is shown in Fig. 6. In the left portion of Fig. 6 the replica is darker (and

thus thicker), in correlation with a large shadowing angle as indicated by short shadows from the polystyrene spheres, while at the right, the photographic density is less, in correlation with the spheres casting longer shadows.

Whether or not a feature on the substrate will cast a shadow depends upon its shape and orientation with respect to the travel direction of the shadowing material. The length of the shadow depends upon both the height of the feature which is casting the shadow and the location and height of the substrate on which the shadow falls. In addition, the shape of the shadow depends not only on the shape of the feature which is casting the shadow but also

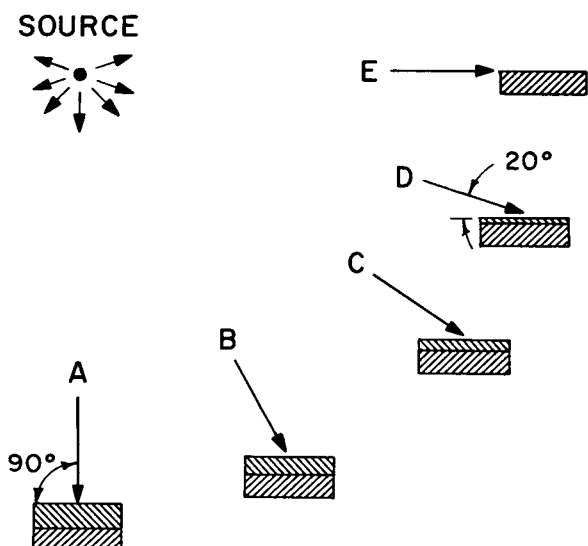


Fig. 5 — The effect of shadowing angle upon the thickness of the deposited film



Fig. 6 — The effect of shadowing angle on the replica thickness. The polystyrene latex spheres on the right cast long shadows and those on the left cast short shadows, corresponding with a thicker shadow deposit and darker image to the left. (Original magnification, 6000X.)

on the shape of the surface upon which the shadow falls.

Figure 7 illustrates the effect of air pressure in the bell jar, during shadowing, upon the sharpness of the shadow. The shadows cast at 2×10^{-5} mm Hg (Fig. 7a) are much sharper than those cast at 5×10^{-4} mm Hg (Fig. 7b). The graininess of Fig. 7b is probably due to the excess thickness of this replica. The magnifications are the same.

Figure 8 shows a sketch of a substrate which is first shadowed at 45° and then rotary-shadowed with carbon to give a more uniform layer of carbon over the whole substrate. The cubic hill (A) and cubic hole (B) may be thought of as either the fracture surface or a plastic replica. On the other hand a hole as at B may be considered a negative plastic replica of a hill as at A in a metal surface, and *vice versa*. The vertical thicknesses of the replica at T_2 are sufficient to prohibit the passage of electrons (even though the actual replica thickness at section Z-Z is equal to T_1), so the outlines of the cubes are black. This sketch illustrates an important point: *features that contain their own shadows were holes at the time of shadow deposition, while features that cast shadows outside themselves were hills*. When one looks at a fractograph, he must be certain of the replication technique used in order to determine whether the feature on the original fracture surface was a hill or a hole. If it is a two-stage (negative) replica, and the feature casts an external shadow, then he is sure that the feature was a hill in the negative replica and a hole in the original surface.

It is seldom, however, that one sees such simplified features on fracture surfaces. Intergranular fractures are frequently encountered, and these are a bit more complex to analyze. Fracture along equiaxed grain boundaries presents more or less flat surfaces to view. Figure 9 shows a system of flat facets which fit together at angles to form a faceted hill (A) and a similarly faceted hole (B). Again this was shadowed at 45° , and then a uniform thickness of carbon was deposited. The effect of the angle of the substrate with the depositing vapor direction is seen in the decreasing replica thickness from T_2 , where the facet is perpendicular to the depositing material direction, through T_5 . At the T_5 positions the facets are essentially parallel

to the vapor direction, and neither the hill nor the hole casts a shadow. The sketch of the fractograph at the top of Fig. 9 shows that not only the angle of the substrate with respect to the direction of travel of the vapor as projected on a vertical plane (α) is important but the angle as projected on a horizontal plane (β) is equally important. Thus the decreasing densities of the facets from X_1 to X_4 are dependent upon both angles.

A fractograph of an intergranular fracture in sintered tungsten of 90% density (5) is shown in Fig. 10a. This fractograph illustrates some interesting points of interpretation. First the intergranular facets are rather flat and therefore of uniform density. *Surfaces which were flat when shadowed and remain flat in the electron microscope have even photographic densities throughout each surface*. If the facets were oriented at different angles to the shadowing direction, then the fractograph density will vary from one facet to another. Facets of equal shadowing angle will have equal densities, provided that their angles with respect to the electron beam are also approximately the same. Figure 10a was made from a negative replica, and one may see that the replicas of the roughly hemispherical holes (sintering pores) at E through G cast shadows outside themselves. The fractograph is repeated in stereo (Fig. 10b) in case some reader wishes to investigate these points himself.* The central portion of the fractograph is a replica of a hole where a grain had been pulled out of the surface. Thus the negative plastic replica is a hill and casts the external shadow at H. Facets A and B are sides of this hill. One can see from the shadowing direction (toward the upper left) that facet A was exposed to the shadowing material while facet B was hidden from the shadowing material. From consideration of the thinner layer of material that was deposited on facet B, one would expect facet B to be lighter than facet A. It is not, however, because its angle with respect to the electron beam direction in the microscope is more acute than that of facet A, and it is tilted in the range (some 60° or 70° away from normal

*Unaided visual stereo viewing is discussed in Appendix A with reference to Fig. 33. One may wish to pause here and practice doing this.

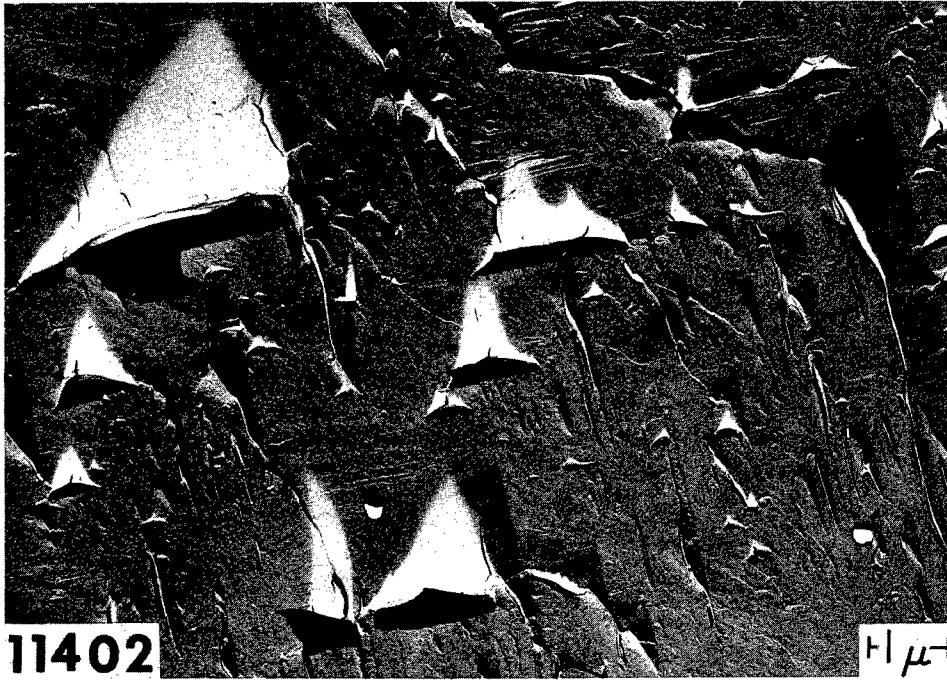
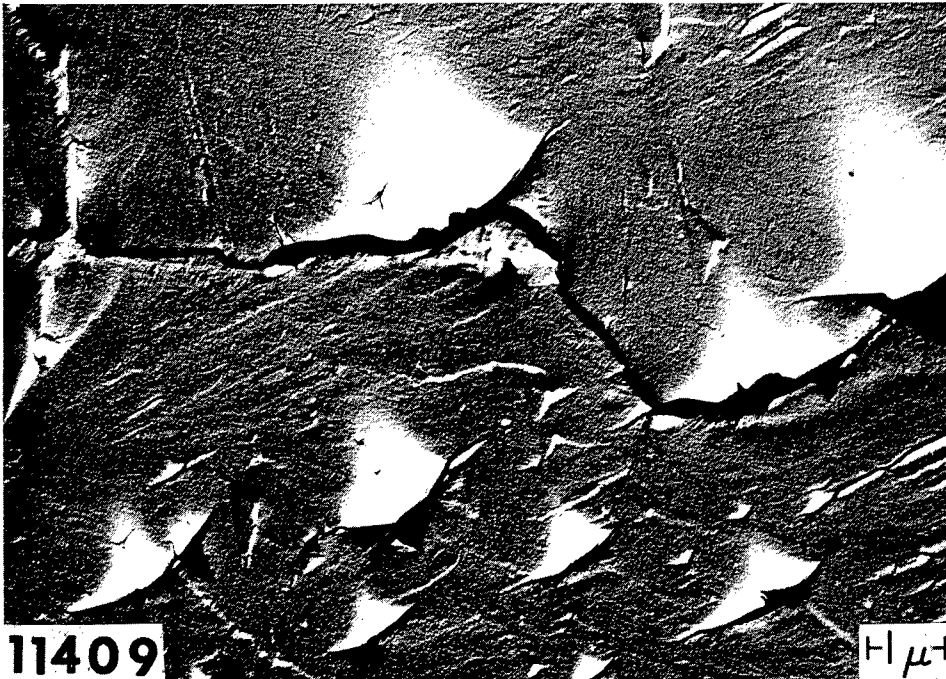
(a) 2×10^{-5} torr(b) 5×10^{-4} torr

Fig. 7 — Effect of air pressure in the bell jar during evaporation on the sharpness of the shadow. This is a two-stage (cellulose acetate-carbon) replica of cleavage tongues in iron. (Original magnification of both photographs, 15,000X.)

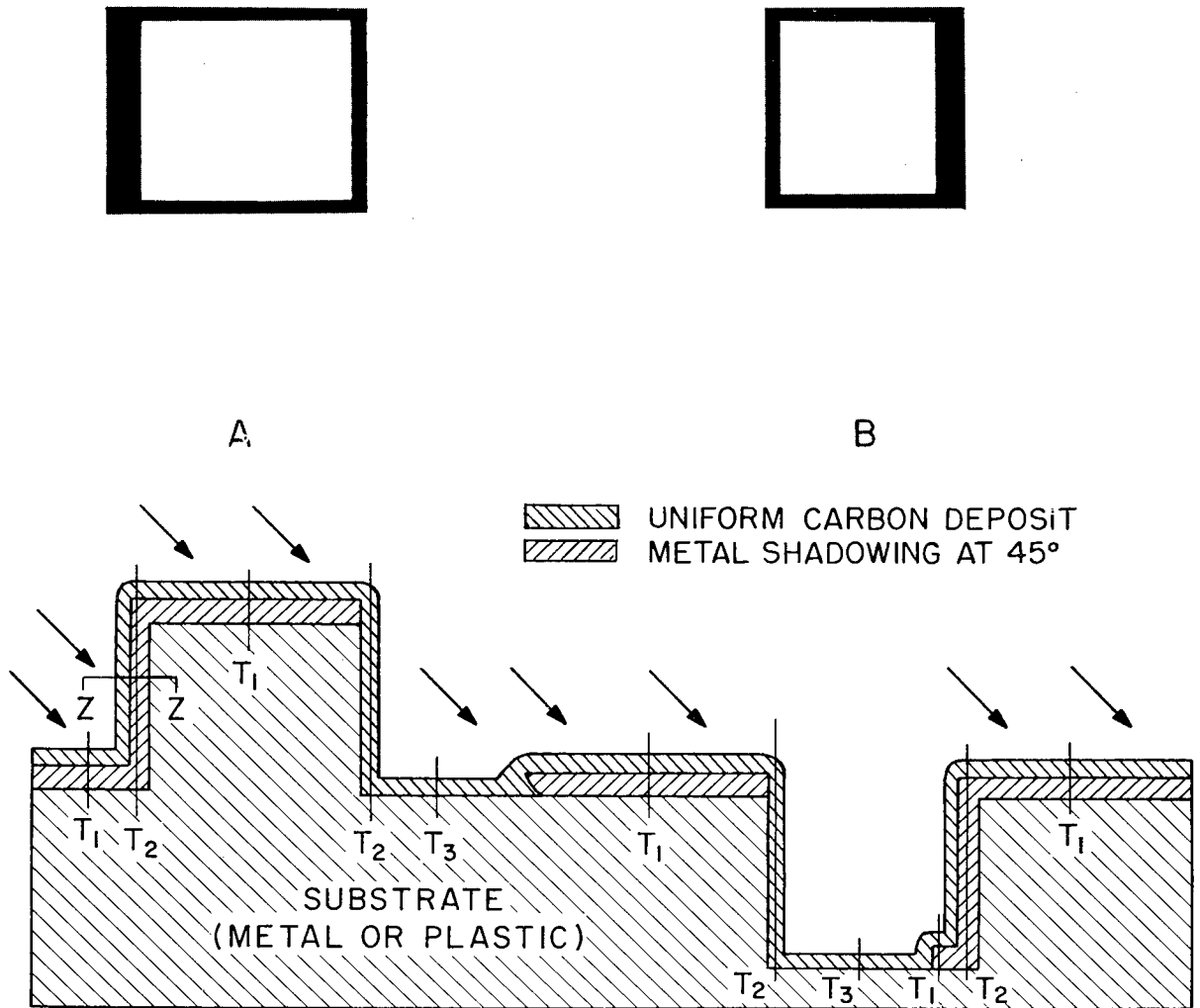
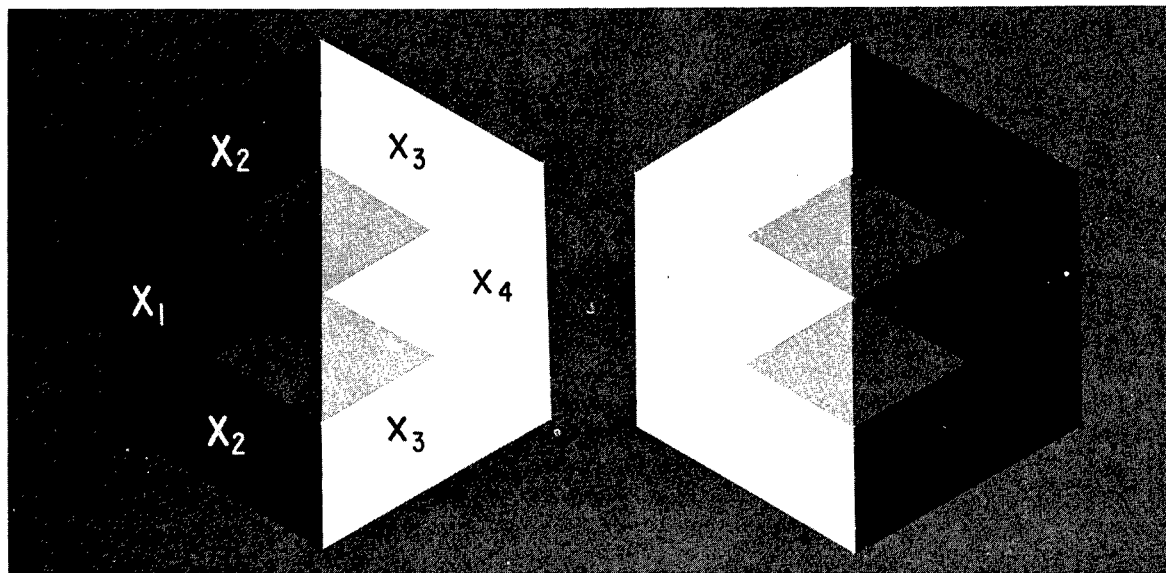


Fig. 8 – Model of the shadowing and carbon backing of features simplified as a cubic hill and a cubic hole. The replica thickness at T_2 locations completely inhibits the passage of electrons; hence an opaque border is seen around the two cubic features at the top. The hill casts a shadow outside the border, while the hole contains its shadow within the border.

to the beam) where the scattering due to this effect is more than scattering due to the film thickness. Facets C and D have approximately the same angle with respect to the electron beam and thus the shading correlates with the deposited film thickness. Facet D was shadowed while C was hidden; thus D is darker than C.

A further example of the effect of the angle between the replica and the electron beam may be seen by comparing Fig. 11a with Fig. 11b. These two fractographs are mounted for unaided eye stereo viewing, and consideration of the labeled facets shows the effect on the contrast when the replica is tilted by 10° in the stereo

01
02
03
04
05
06
07
08
09
10
11
12
13



A

B

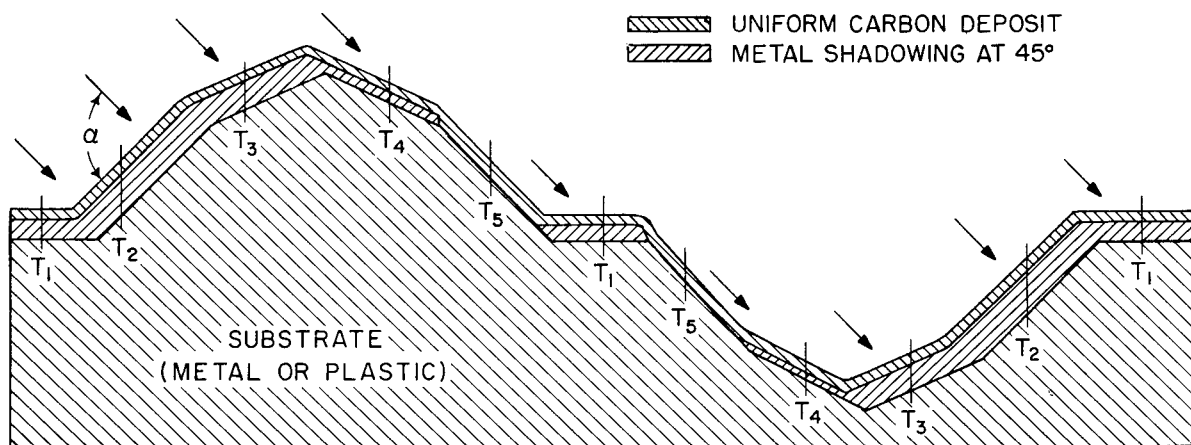


Fig. 9 - More realistic replica shape than in Fig. 8, illustrating many facet orientations, and considerations of the two components of the shadowing angle (α and β)

holder. In (a) the replica is tilted 5° to be viewed more from the left and in (b) it is tilted 5° to be viewed more from the right. Facets A and D appear flat and nearly horizontal when viewed in stereo, which means that in making the two fractographs they were tilted about 5° each way from perpendicularity to the incident electron beam direction. They therefore have about the same density in both fractographs. The angle between the electron beam and facets B and C

increased from Fig. 11a to Fig. 11b; therefore, facets B and C appear lighter in Fig. 11b.

Other examples of flat surfaces are shown in Figs. 12 through 15, with each caused by a different mechanism. The flat facets in Fig. 12 were formed when a titanium alloy was stress-corrosion cracked at room temperature in distilled water. The facets strongly resemble those seen in cleavage of body centered cubic or HCP metals (6). Figure 13 shows a fractograph from

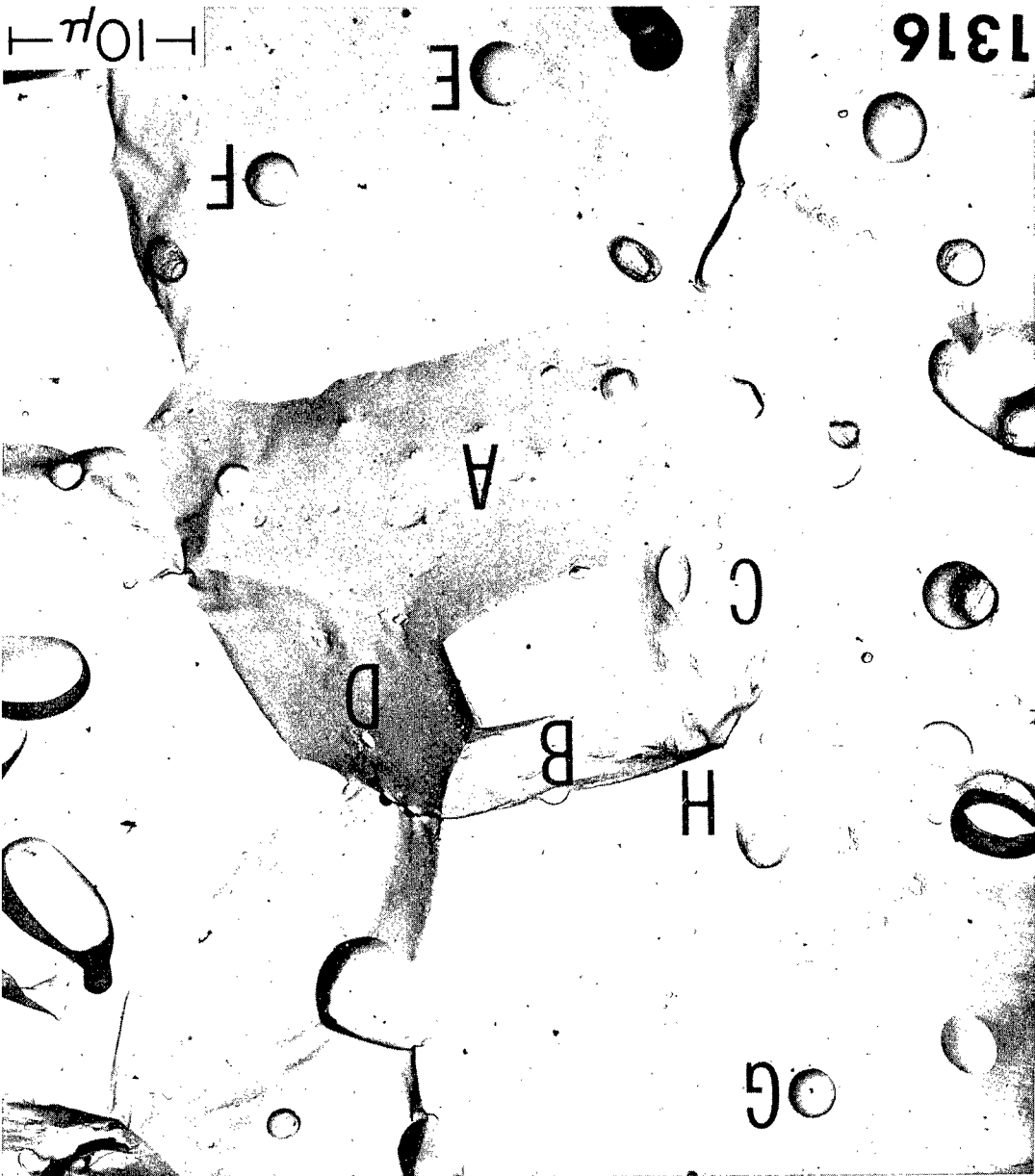


Fig. 10a - Fractograph of an intergranular fracture in 90% dense sintered tungsten. The replica is shadowed with palladium; it was prepared by a two-stage (cellulose acetate-carbon) technique and thus is a negative replica. Regions A through D are grain facets, H is an external shadow, and E through G are sintering pores. The external shadows indicate hills in this negative replica and hence holes in the original surface. (Original magnification, 2700X.)



Fig. 10b - Fractographs of the replica shown in Fig. 10a arranged for stereo viewing

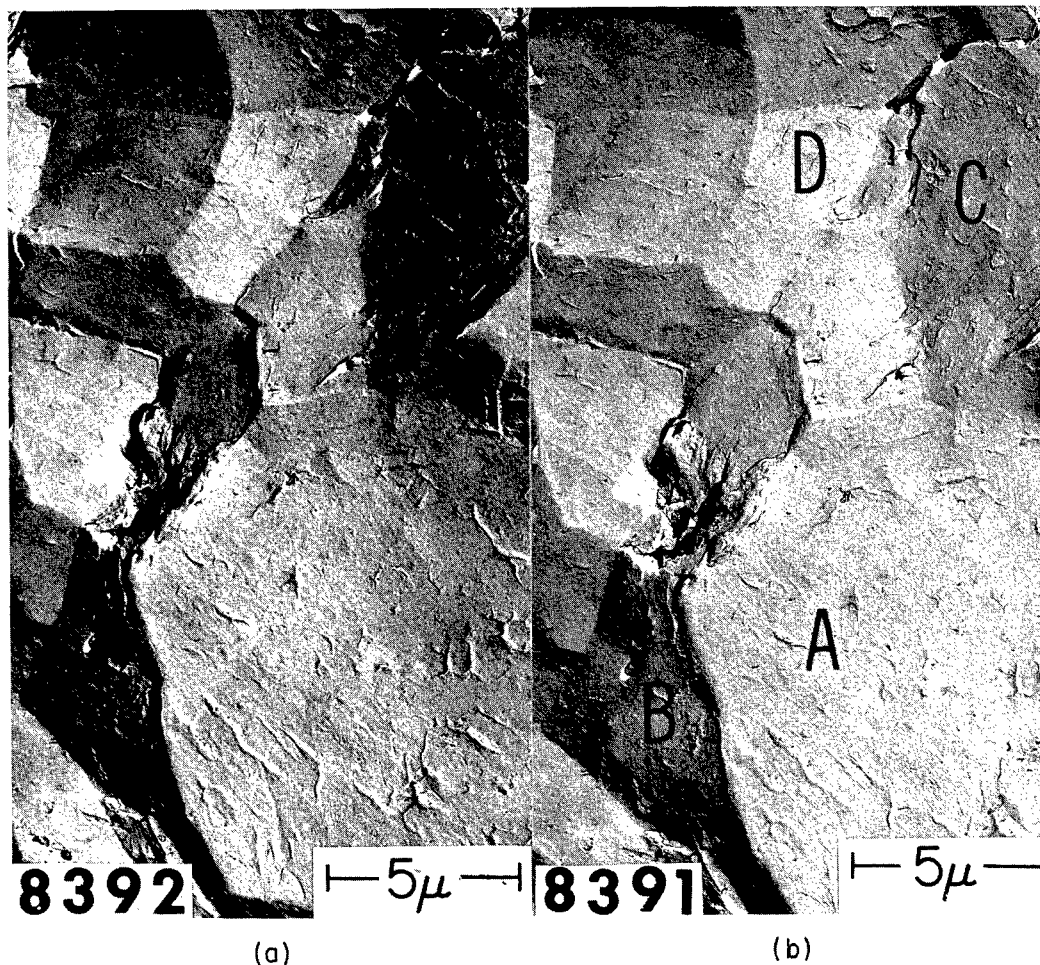
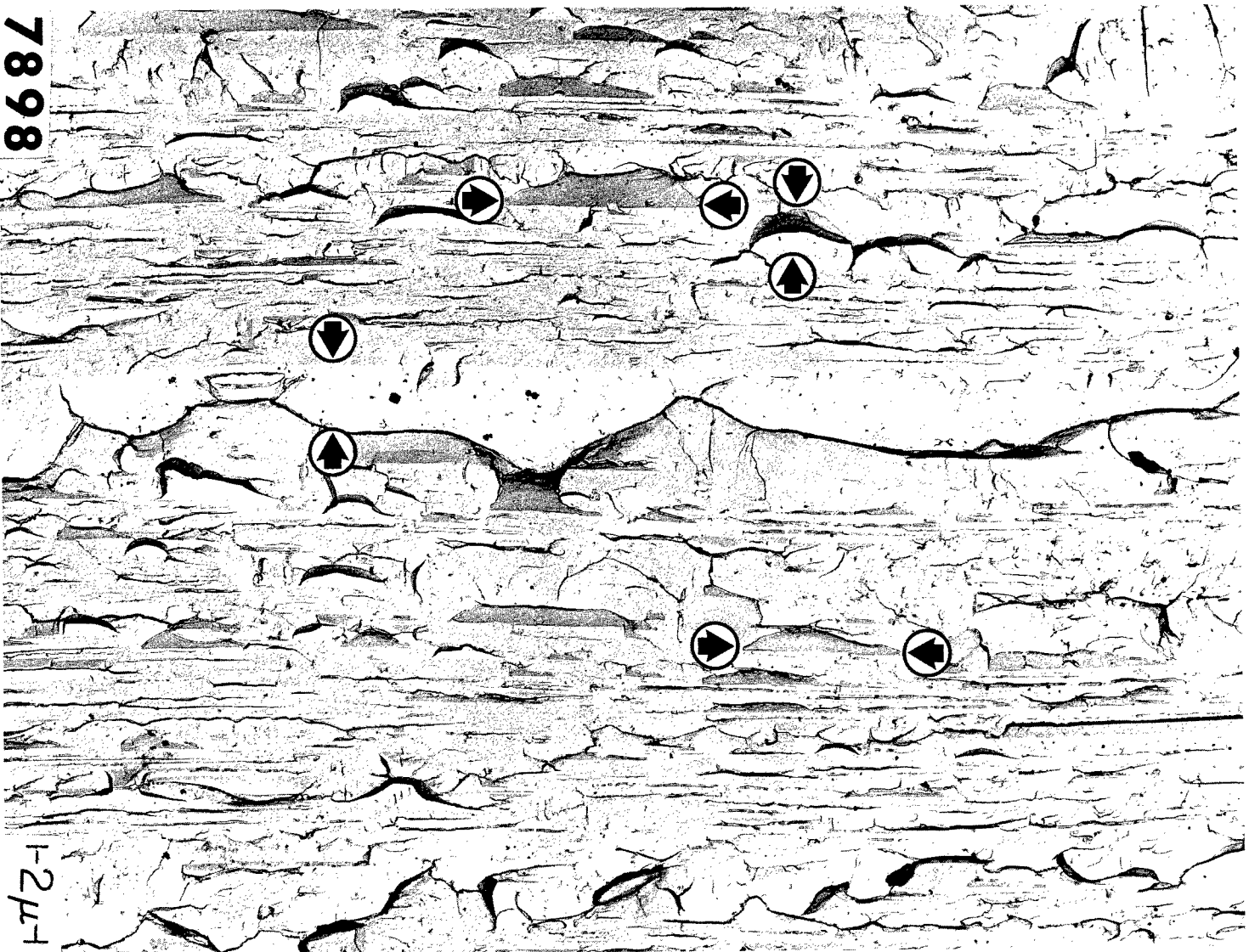


Fig. 11 - Stereo pair of fractographs of a piece of AISI 4340 steel which was stress-corrosion cracked in distilled water. Facets B and C, which in the replica drop down toward the right, are photographically lighter in (b), where the replica is viewed in the microscope more from the right. This is a two-stage (cellulose acetate-carbon) replica. (Original magnification, 6000X.)



Fig. 12 - Cleavage, due to room temperature stress-corrosion cracking, in a Ti-7%Al-2%Nb-1%Ta alloy. This is a two-stage (plastic-carbon) palladium-shadowed replica. (Original magnification, 6000X.)



7898

1-2μ

Fig. 13 - Cleavage in iron, showing three different facet orientations. This is a palladium-shadowed direct carbon replica. (Original magnification, 9000X.)

01
02
03
04
05
06
07
08
09
10
11
12



Fig. 14 – Secondary cracks with a probable crystalline orientation effect upon fracture path in the fatigue of a 2024-T851 aluminum alloy. This is a two-stage (cellulose acetate-carbon) palladium-shadowed replica. (Original magnification, 6000X.)

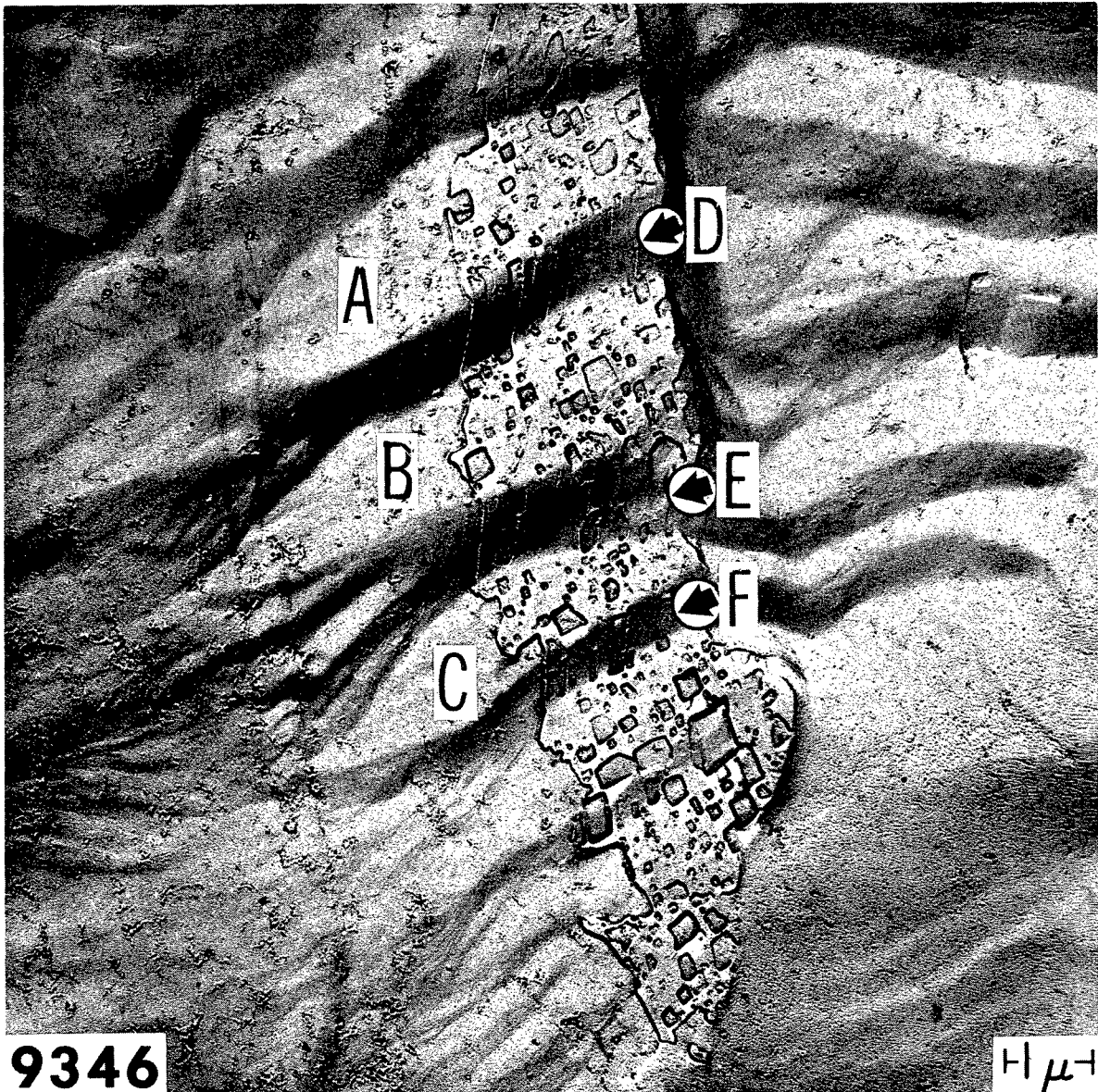


Fig. 15 - Slip steps in iron deformed at room temperature after it had been etch-pitted. The light surfaces A, B, and C are mutually parallel and represent an originally flat surface which was dissected by slip. This is a two-stage (cellulose acetate-carbon) palladium-shadowed replica. (Original magnification, 15,000X.)

an iron specimen which was cleaved at dry ice temperature. Cleavage facets of three orientations may be seen: the major portion of this region is at one orientation, while smaller facets are seen to be either lighter (examples between horizontal arrows) or darker (examples between vertical arrows). The three orientations have distinct densities, with all the facets of a given

orientation having consistent density. Figure 14 shows the effect of crystal orientation on fatigue fracture surface markings. The overall fractograph shows one orientation, while frequently the fatigue crack has propagated along portions of another set of planes (examples between the arrows). The effect of crystal structures on producing flat surfaces is further seen in Fig. 15.

Here a region on the surface of an iron wire was polished, etch-pitted, and then bent (7). The alternating light and dark parts of the central portion shows where slip on parallel planes dissected the patch of etch pits. Surfaces A, B, and C are the original surface (unstrained), while D, E, and F are new surfaces formed during the slip process. Surfaces A, B, and C are mutually parallel and have the same photographic density. The same is true for the new surfaces D, E, and F.

One must exercise extreme care in his interpretation, however, when determining which surfaces are parallel. The indicated surfaces in Figs. 13 through 15 are known to be parallel because many fractographs were analyzed in stereo. It should be remembered that the same

density in two regions of a fractograph is no guarantee that these regions were at the same angle during shadowing or were at the same angle with respect to the beam in the microscope.

Figure 16 illustrates the deposited material thickness and image appearance of convex and concave curved surfaces. Although the heights and depths illustrated are not sufficient to cast shadows, the photographic density tends to be darkest where the replica is locally oriented most nearly normal to the direction of the depositing material. The dashed line *a* across the sketch of the fractograph indicates the line of constant density which one would expect from the shadowing angle, and this is what one sees on fractographs when the height of the curved surface is small in relation to its diameter.

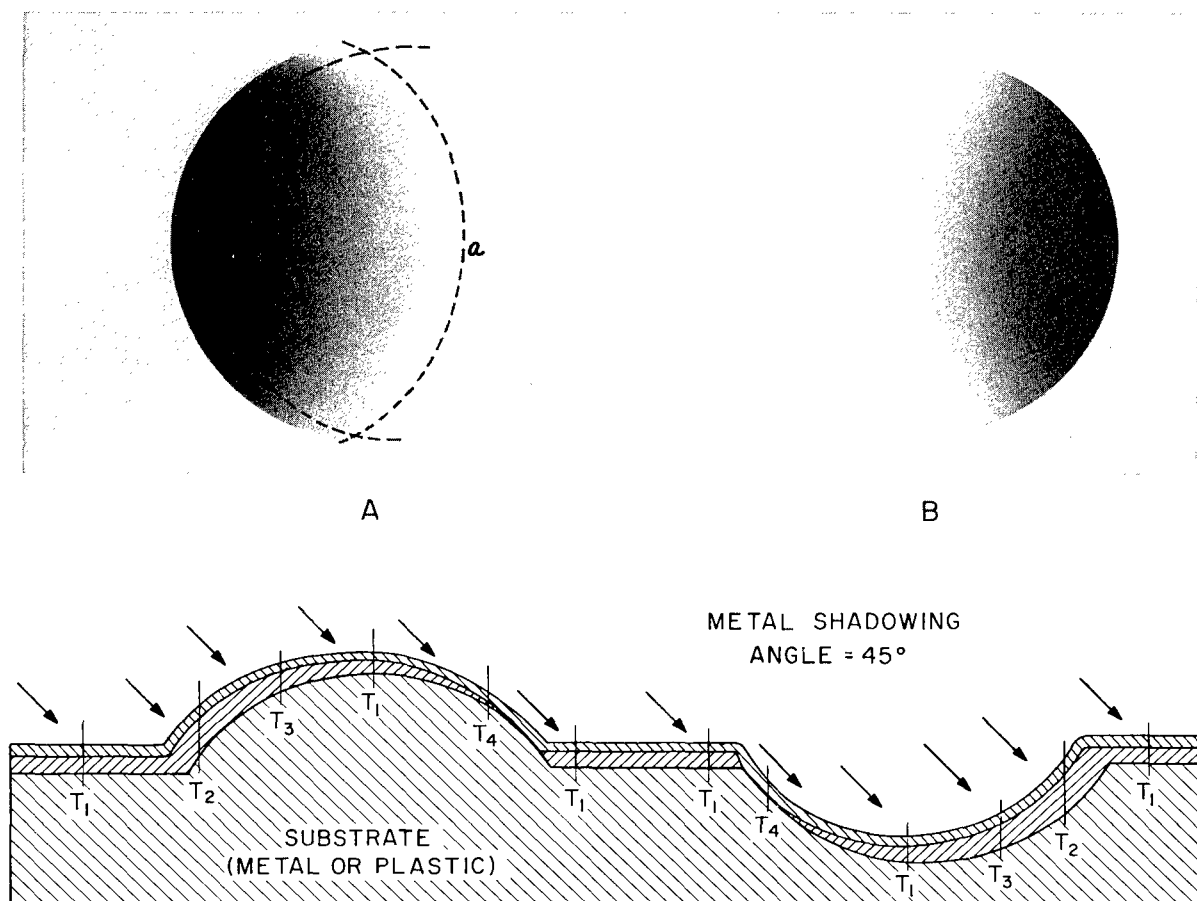


Fig. 16 — Simplified sketch of a curved convex hill (A) and a concave hole (B). The dashed line *a* at the upper left represents a line of constant density which one would expect from considerations of the shadowing angle, while *b* is the line of constant thickness as would be seen vertically by the microscope when the hill is high with respect to its radius.

When the height approaches half the diameter, however, the edges of the rounded feature become nearer vertical, and the density which one sees on the fractograph becomes predominantly affected by the angle of the replica surface to the incident electron beam. A line of constant density in this case would be more like the dashed line *b* in Fig. 16. Examples of this effect are seen in the negative replicas of hemispherical holes in the fractograph shown in Fig. 10a, where E and F have lines of constant density as sketched as line *b* in Fig. 16. Pore G shows constant density at equal distances from its center because the scattering of the electrons is more dependent upon the angle of the replica with respect to the electron beam than it is upon the local shadowing metal thickness.

Both Figs. 16 and 17 illustrate another rule in interpretation: *gradually changing density means that the surface is a curved surface in the microscope or that the replica was flattened after shadowing.* Figure 17 shows a direct carbon replica of a tough pitch copper fracture surface. The three straight lines span three concave dimples (between arrows) which resulted from plastic flow and the coalescence of voids. Shadowing direction is from lower left to upper right. Inspection of the density along any of the three lines shows it to be gradually changing. Other dimples in a more heavily shadowed replica of another fracture surface (Fig. 18) show this gradual change of density more clearly.

Figures 19, 20, and 21 illustrate the fact that flat surfaces on the fracture surface may appear as regions of gradually changing density in the fractographs. Figures 19 and 21 are replicas of cleavage surfaces which are known to be composed of flat facets. The replica shown in Fig. 19 is of iron cleaved at dry ice temperature and shows where the replica has broken and curled as sketched in Fig. 20. The gradual change in density is seen between the arrows (Fig. 19). Figure 21 shows a replica of a cleaved single crystal of tungsten, with flat surfaces on the original specimen shown between the vertical arrows (8). The horizontal arrows show where the replica wrinkled on the grid. Thus, when one sees a region of gradually changing density, he knows the surface was either rounded during shadowing, or was rounded in the microscope, or both. He thus must ask himself, "When was

it rounded?" This will be discussed further in a later section of the report.

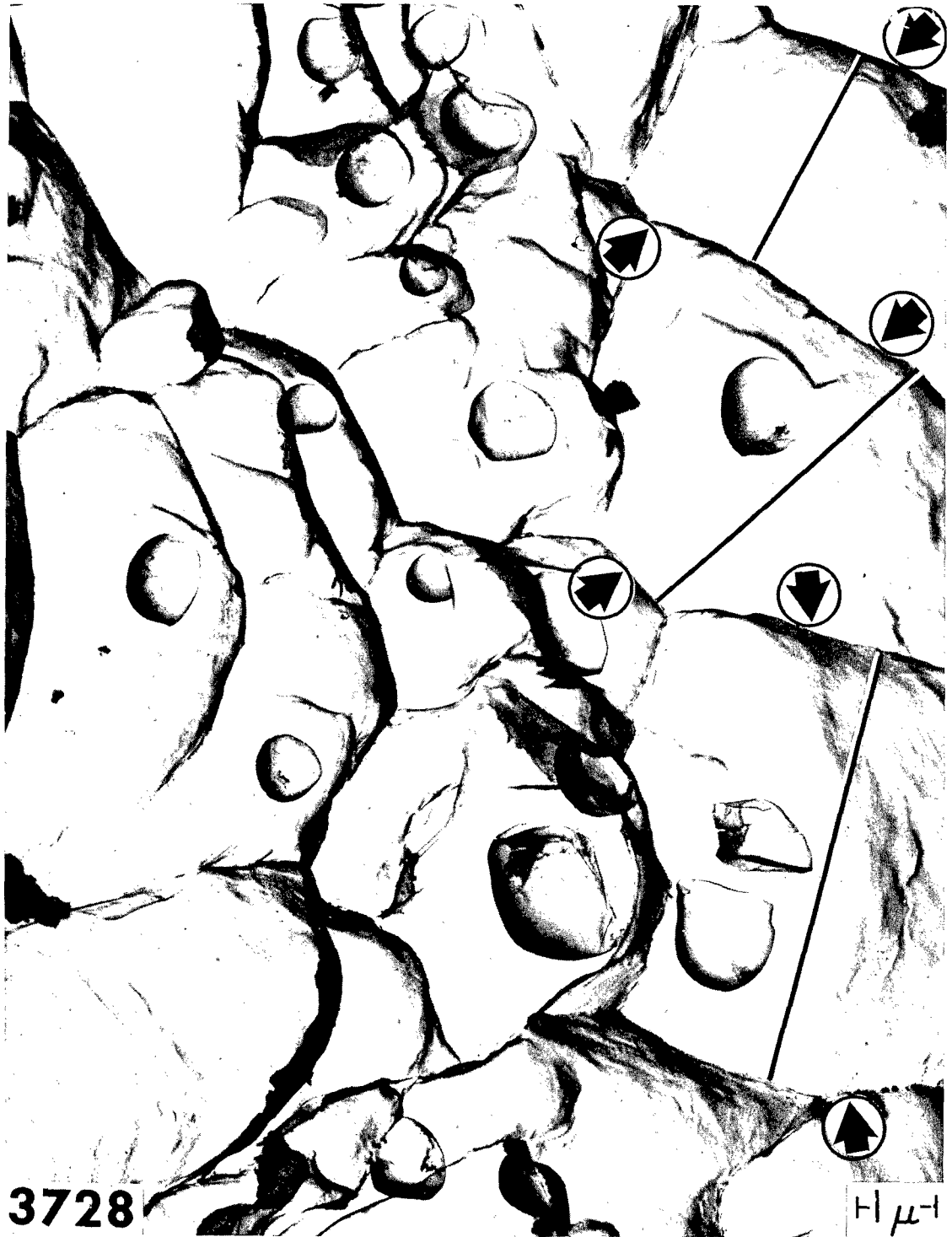
Artifacts

In fracture surface studies, a general rule is to observe the fracture surface itself if possible. If this is not possible, due to demands on magnification or for some other reason, and a replica must be made, the general rule is to make a direct replica of the surface. The use of a two-stage process is often necessary, however, and some have used three-stage processes. The further one gets from direct observations of the fracture surface, however, the more trouble he is likely to encounter from the presence of features on the replica that are due to replication factors alone. These structures that are not related to the fracture processes are called artifacts, and proper analysis of fracture mechanisms depends upon the proper identification of these artifacts. Sometimes the artifacts can be so numerous as to completely hide the shape of the original fracture surface. Thus artifacts must be either identified, or both identified and eliminated, depending upon how much they hinder the collection of meaningful observations.

In the range of magnifications where the light microscope can be used to study fracture surfaces, its use is essential to proper analysis. Figure 22 shows the difference between light microscope and electron microscope pictures of the same region on a surface in which a low-cycle fatigue crack has initiated (7). The light microscope distinctly shows the crack, whereas the electron microscope fractograph gives little indication of a crack.

Figure 23 shows an extreme example of poor replica fidelity. The dimpled fracture surface was first replicated with a room-temperature-setting silicone rubber. This was then replicated with parlodion in amyl acetate, and the parlodion replica was placed in the evaporator and a carbon replica made of it. Though the poor resolution is due largely to the poor choice of the particular rubber used to make the first replica, it is still a good general rule to use as few replicating steps as possible.

Other, more common, artifacts are shown in Figs. 24 through 28. Figures 24 and 25 show undissolved plastic or other partially dissolved



3728
Fig. 17 – Direct carbon replica of dimples (depressions shown between arrows) in tough pitch copper. The palladium shadow direction is from lower left to upper right. (Original magnification, 15,000X.)

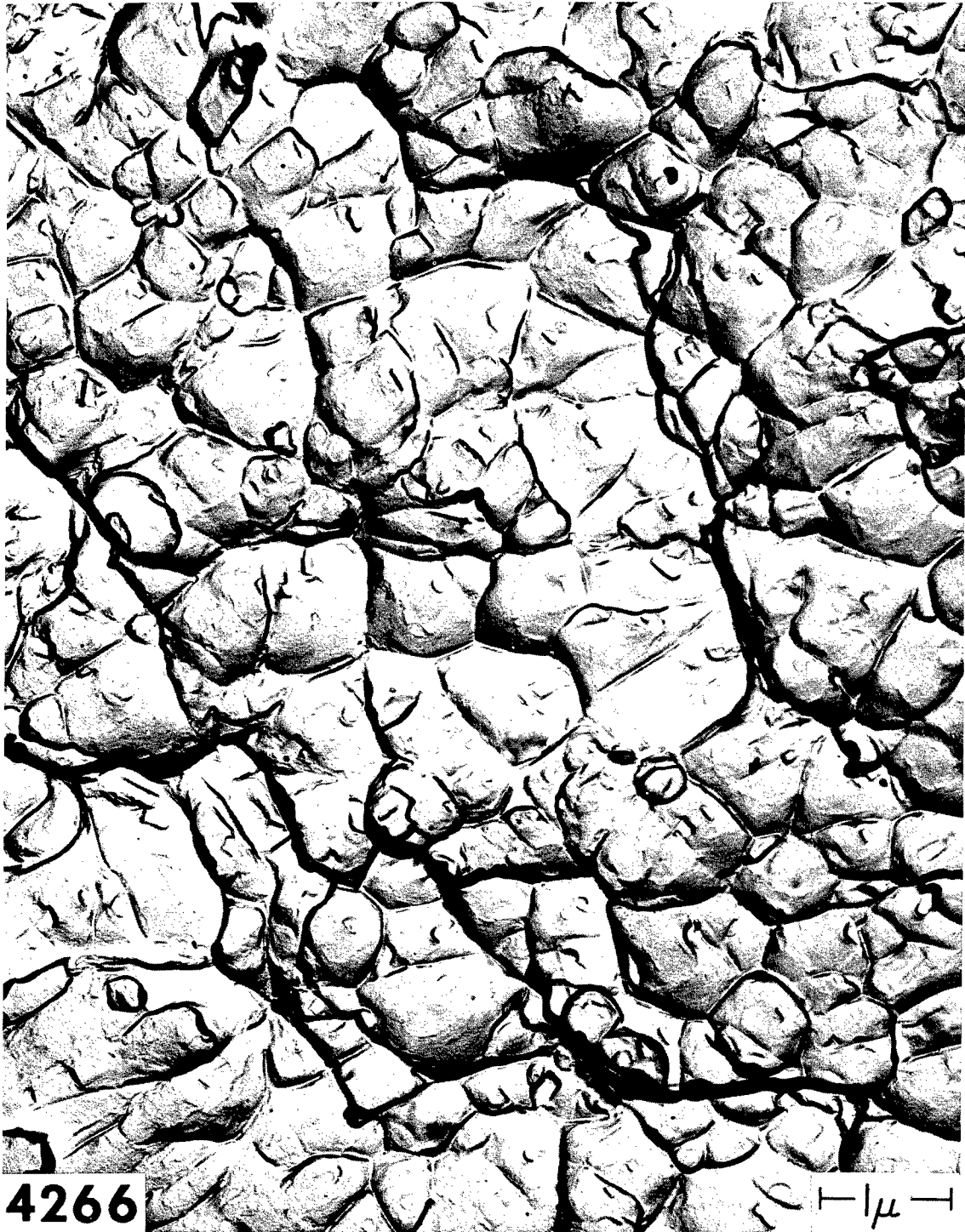


Fig. 18 - Dimples in maraging steel. This is a two-stage (cellulose acetate-carbon) palladium-shadowed replica. (Original magnification, 25,000X.)

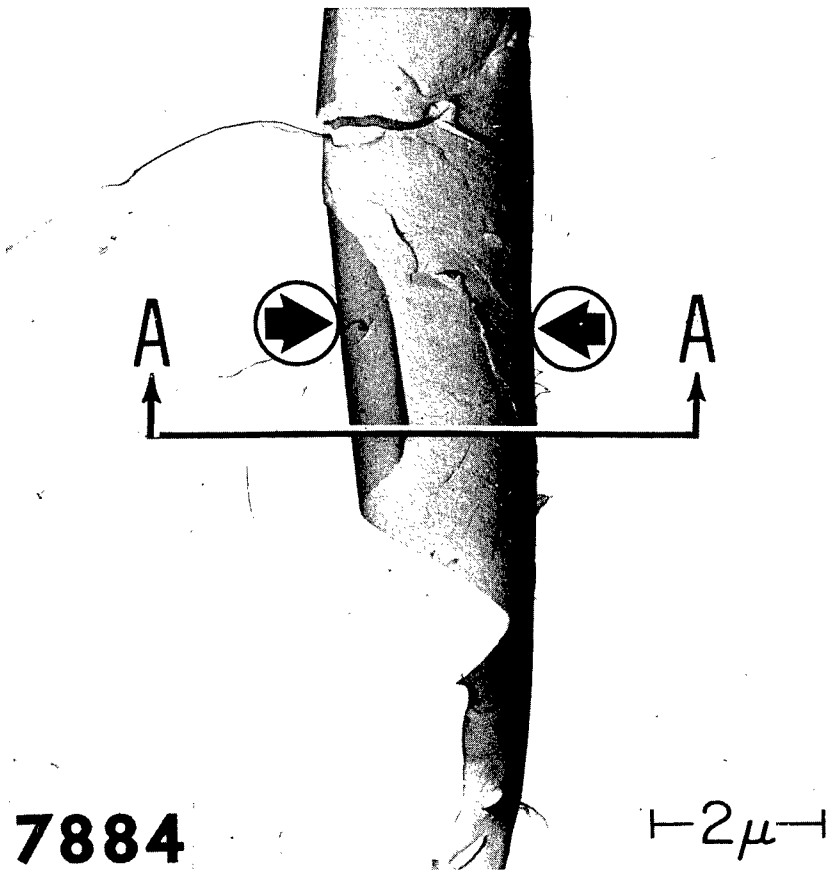


Fig. 19 – A torn and curled portion of a direct carbon replica of a flat fracture surface (iron cleaved at dry-ice temperature). A region of gradually changing density is shown between the arrows. Section A-A is sketched in Fig. 20. (Original magnification, 12,000X.)

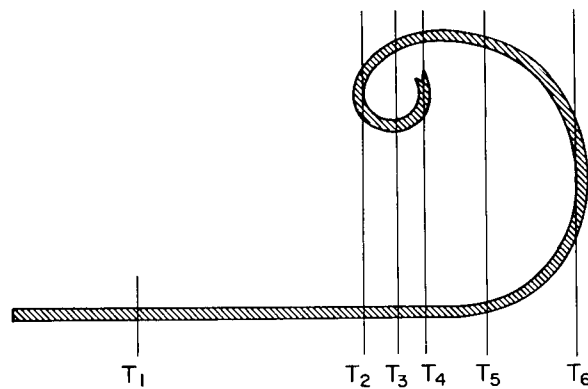


Fig. 20 – Section A-A of Fig. 19. Thicknesses T_2 , T_1 , and T_6 are sufficient to stop the electron beam.

011
012
013
014
015
016
017
018
019
020

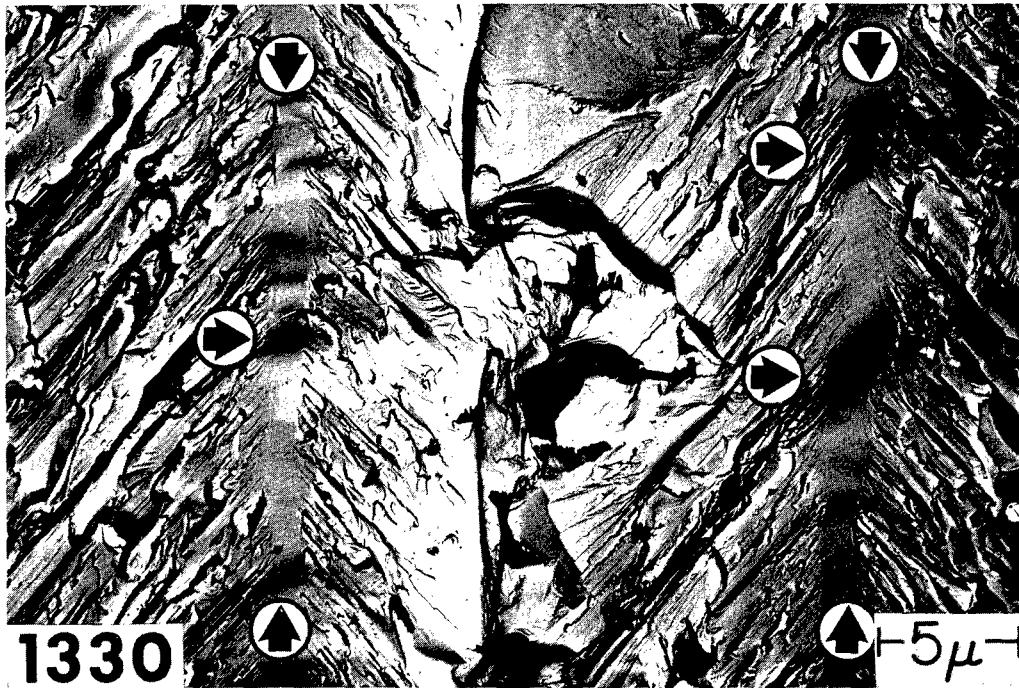


Fig. 21 – Cleavage in a tungsten single crystal (8). The vertical arrows indicate originally flat surfaces, while the horizontal arrows indicate wrinkles in the replica. This is a two-stage (cellulose acetate-carbon) palladium shadowed replica. (Original magnification, 4000X.)



(a) Light microscope



(b) Electron microscope

Fig. 22 – A comparison of light microscope and electron microscope pictures of a fatigue crack trough. The trough is easily seen in (a), where the focus is a function of depth, but the identical region might escape detection in (b), where the clarity is not a function of depth. (Original magnification, 650X.)

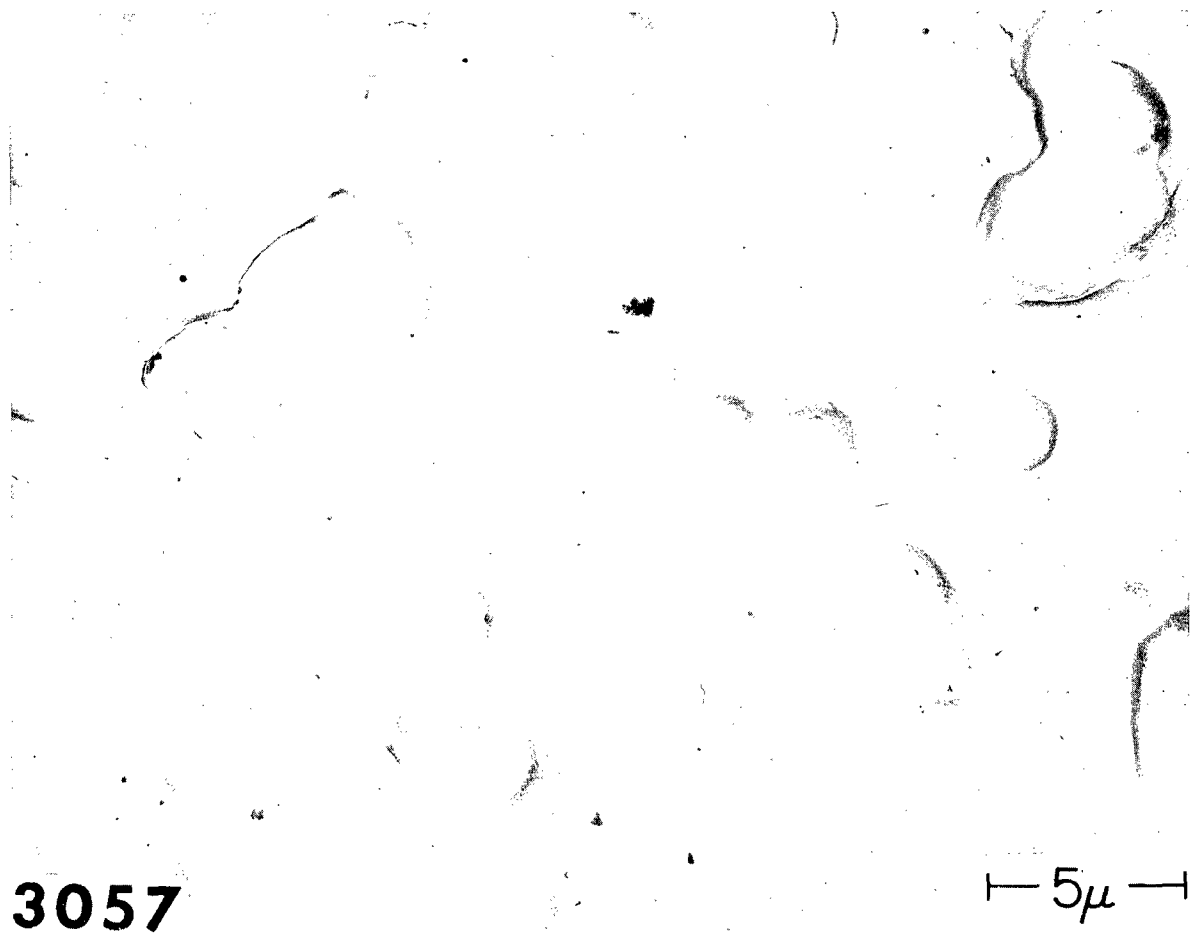


Fig. 23 — Replica showing poor fine-scale fidelity. A three-stage replication technique was used, with a poor grade of room-temperature curing rubber as the first replica. (Original magnification, 6000X.)



Fig. 24 - Example of incompletely removed plastic from the carbon in a replica made by the two-stage, cellulose acetate-carbon technique. (Original magnification, 6000X.)

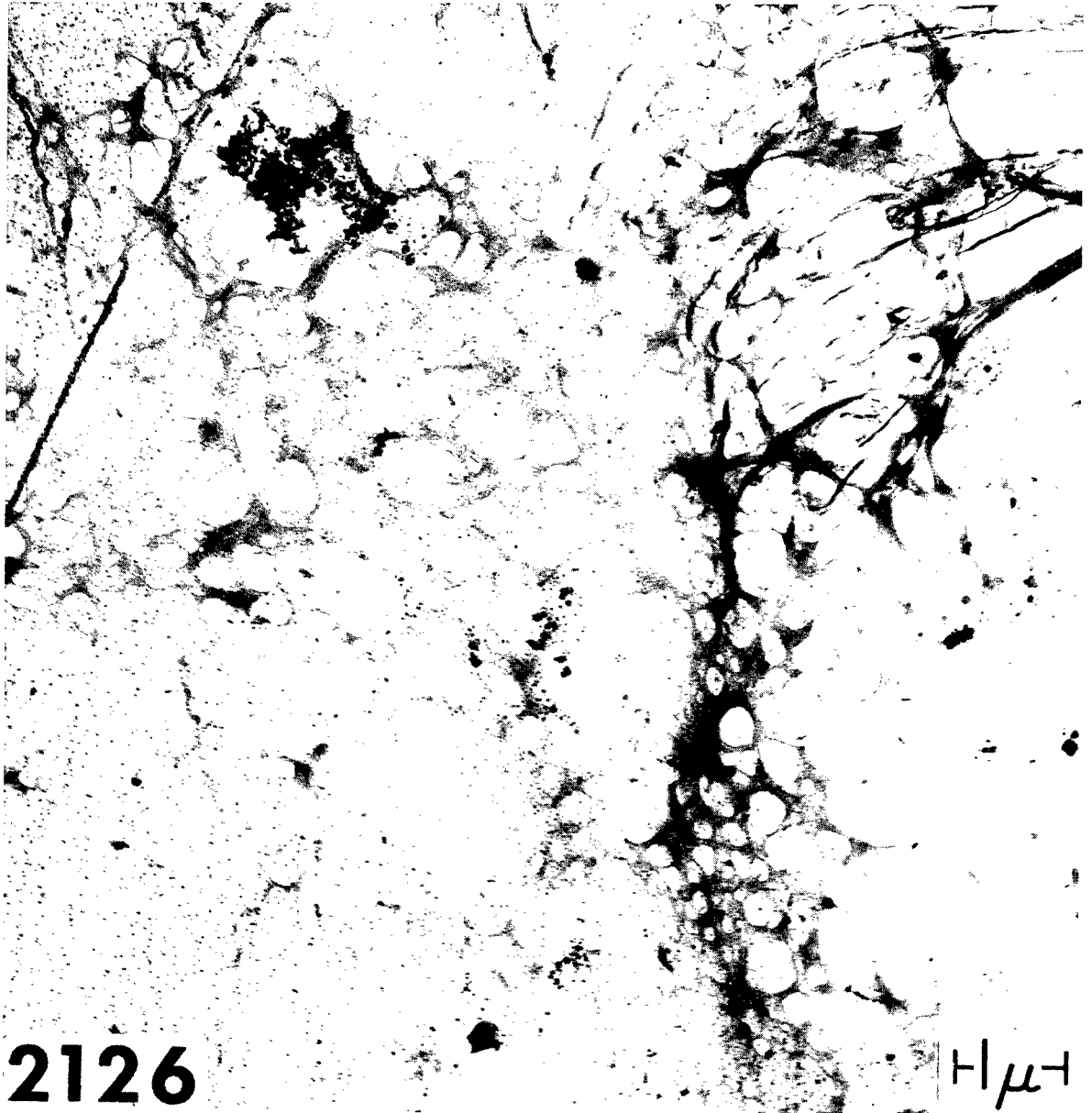


Fig. 25 – Another example of incompletely removed plastic from the carbon in a replica made by the two-stage, cellulose acetate-carbon technique. (Original magnification, 14,000X.)

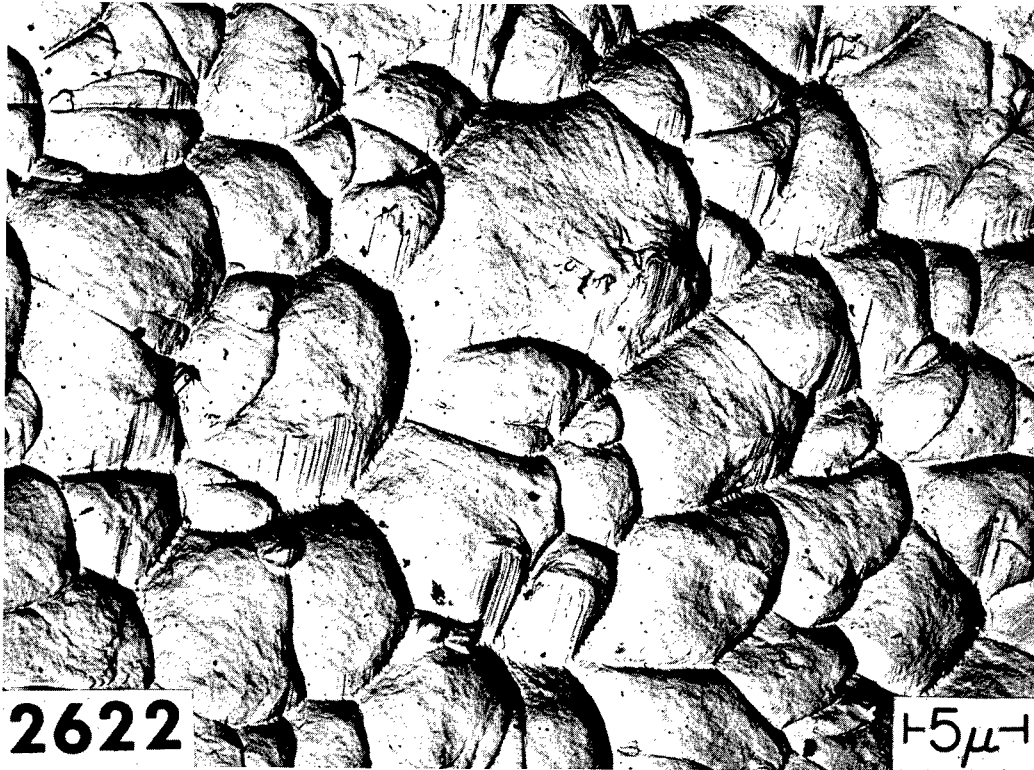


Fig. 26 – Scraping artifact frequently encountered in the two-stage process. The markings are formed when the plastic is scraped against some portion of the specimen during removal from the specimen. (Original magnification, 3500X.)

organic substance (glue from tape is a possibility). Figures 26 and 27 show two artifacts which are inescapable when plastic replicas are made of rough fracture surfaces. The plastic *always* scrapes against some protrusions on the fracture surface as it is removed (Fig. 26). Some plastic inevitably is securely wedged into the crevices and the plastic locally rips apart when the rest of the plastic is removed, leaving small bits of plastic in the crevices. The surface of a tear in cellulose acetate is shown in Fig. 27. The scraping artifacts shown in Fig. 26 and tears in plastic as shown in Fig. 27 have been misinterpreted by several investigators as proof of various fracture mechanisms. Fatigue, glide plane decohesion (slip, producing slip steps), and hydrogen embrittlement are some of the mechanisms which have been "identified" erroneously by not recognizing scraping or tear-in-plastic artifacts. An artifact produced

by scraping may have different appearances, depending upon both (a) how much area of the plastic was dragged across a specimen projection, and (b) how hard it was pressed against the projection as it was scraped across the projection. This scraping artifact generally is on the side of a hill with several or many closely spaced parallel lines extending approximately up and down the hill. Depending on (b) above, these lines may be superimposed upon the real shape of the fracture surface, a combination which can lead to wasted interpretation time if the artifact is not recognized.

Other artifacts have been shown and discussed in Refs. 9 and 10. Figure 28 shows a direct carbon replica where the shadowing material was partially removed and was peeled up in pieces (at arrows) during the electropolishing which was used to free the replica from the fracture surface.

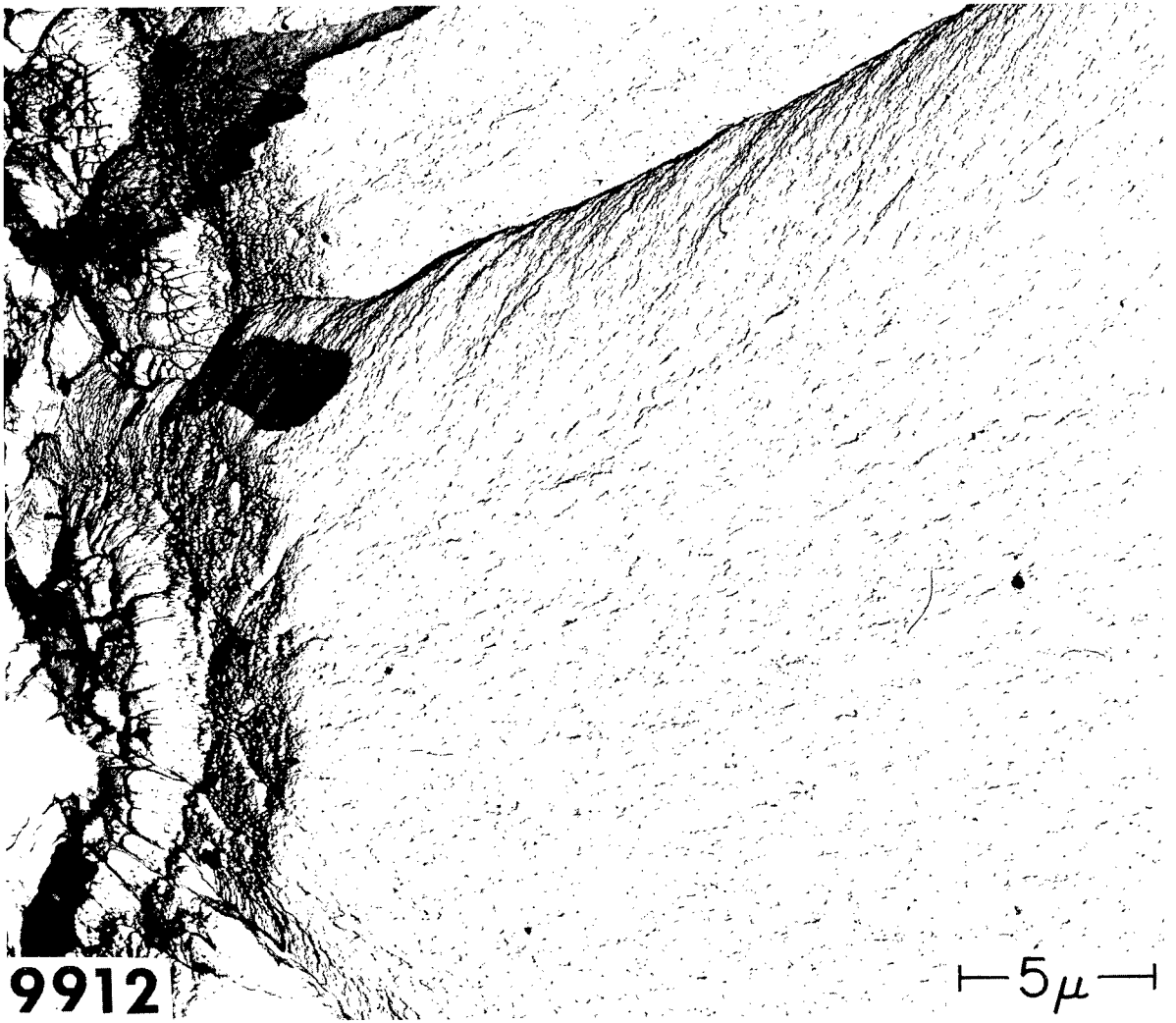


Fig. 27 — Features of torn-plastic artifacts often seen where the plastic is stripped from an extremely jagged fracture. Parts of the plastic replica are so firmly held in the specimen that they tear during stripping. This is a two-stage (cellulose acetate-carbon) replica. (Original magnification, 6000X.)

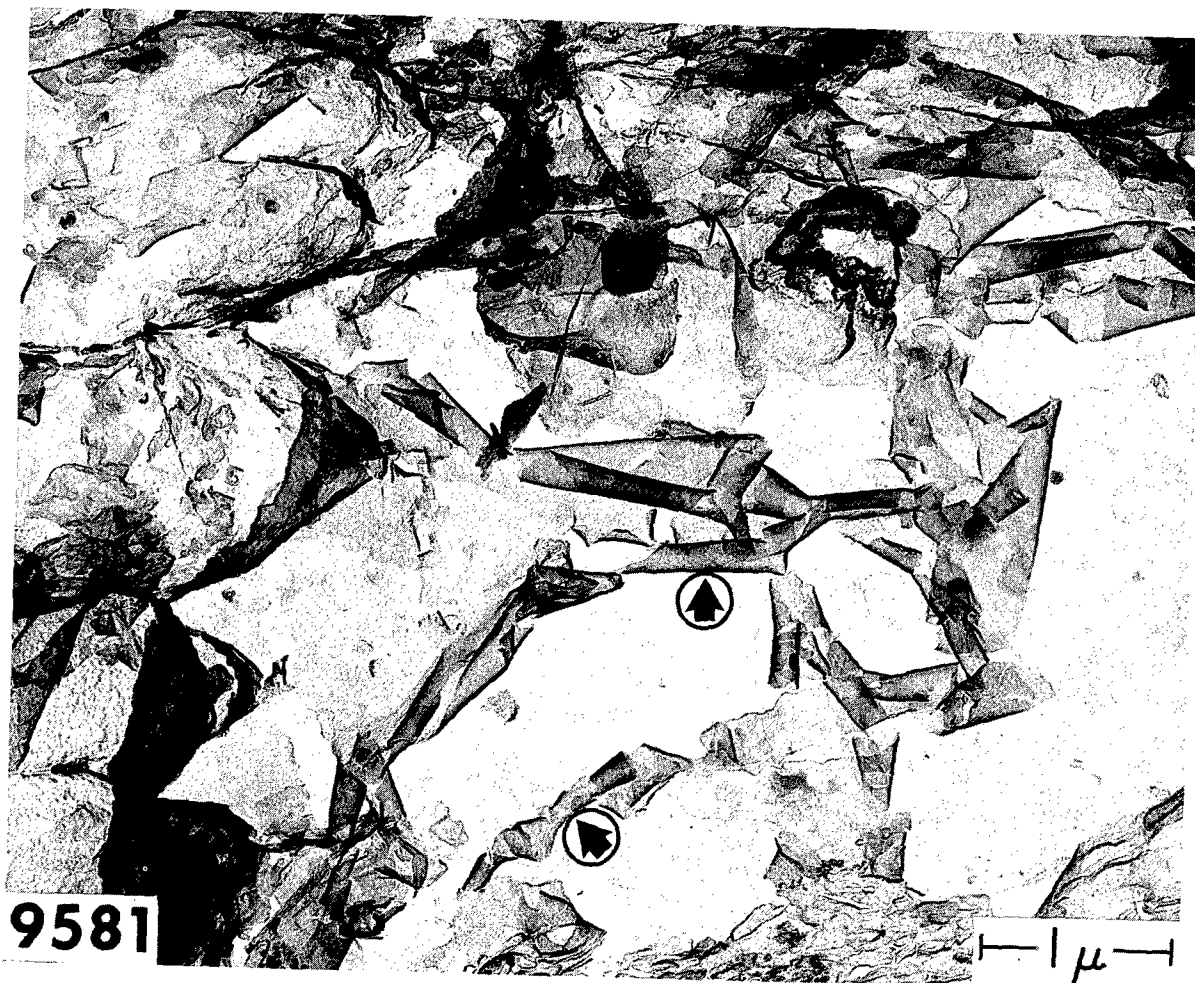
012
013
014
015
016
017
018
019
020
021
022
023

Fig. 28 - Shadowing material (palladium) which was partially removed from a direct carbon replica during the electropolish-freeing process. (Original magnification, 30,000X.)

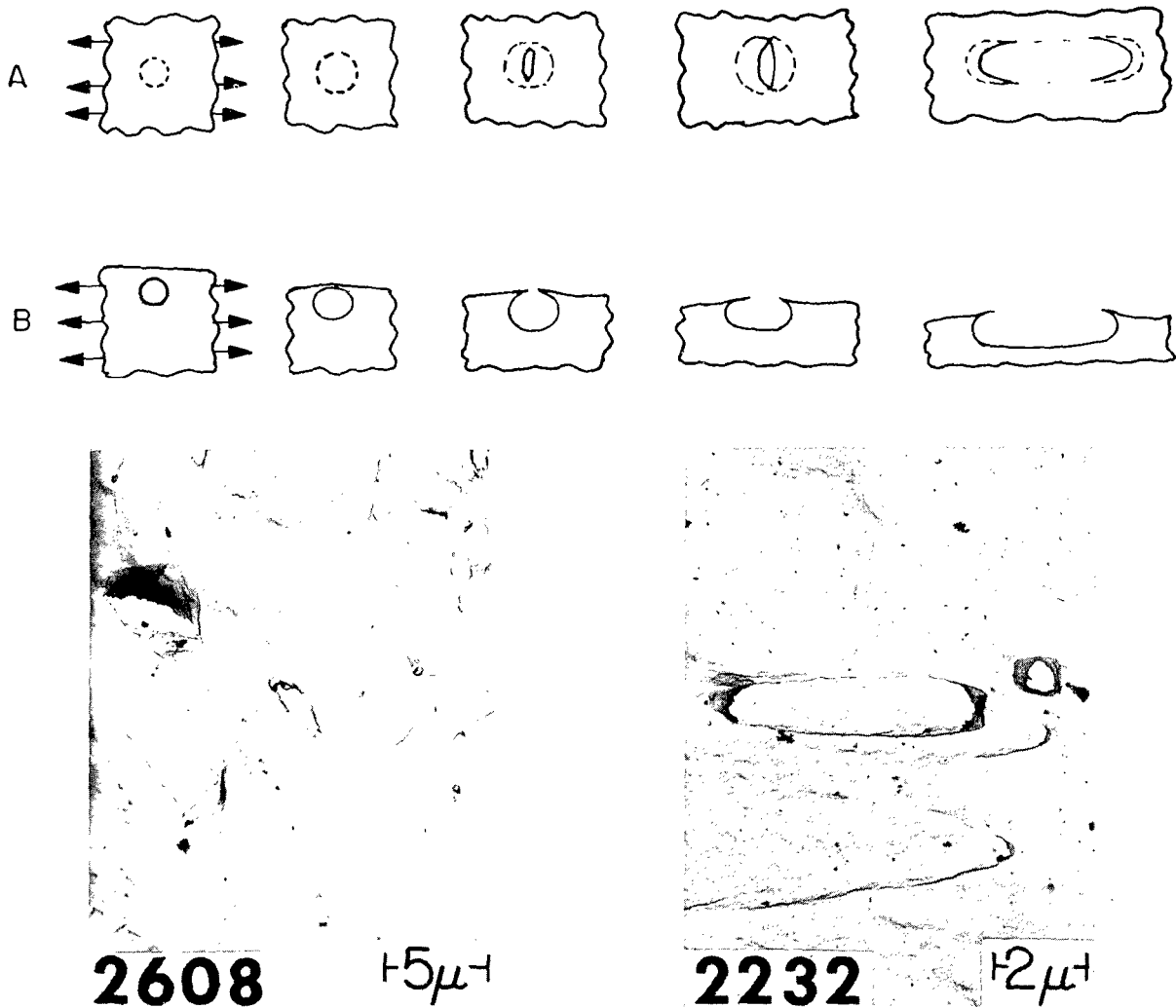


Fig. 29 - Sketch (top) showing stages of formation, and direct carbon replicas (bottom), of tear dimples. The sketch shows the coalescence of a void with a larger free surface, with (A) showing the fracture surface and (B) showing the cross section. The fractographs show iron on the left and 304 stainless steel on the right. (Original magnifications, 3000X on the left and 7000X on the right.)

The problem of maintaining replica fidelity during removal of plastic from fracture surfaces, and the superiority of the direct replication process, is illustrated in Figs. 29, 30, and 31. Figure 29 sketches the formation of the oval dimple (11) and shows examples of direct carbon replicas of this type of fracture surface. The stripping action during removal of plastic from such a fracture surface feature, however, cannot help but deform the plastic, if it can be pulled out at all. Figure 30 shows what happens. Essentially the same thing is shown in Fig. 31, where the top fractograph shows spade-shaped

"tongues" in a direct carbon replica of a cleaved piece of iron, and the bottom fractograph shows the same kind of feature as replicated by cellulose acetate. The arrows in the two fractographs point to the tongues. The plastic at the bottom of the tongues either remained there during the stripping, or was bent up when it was removed from the tongues, because the three thicknesses of carbon shown comprising the tongues in the top are not present in those shown at the bottom.

Another common artifact is shown at E in Fig. 32. This is simply a local ripping apart and partial overlapping of the replica.

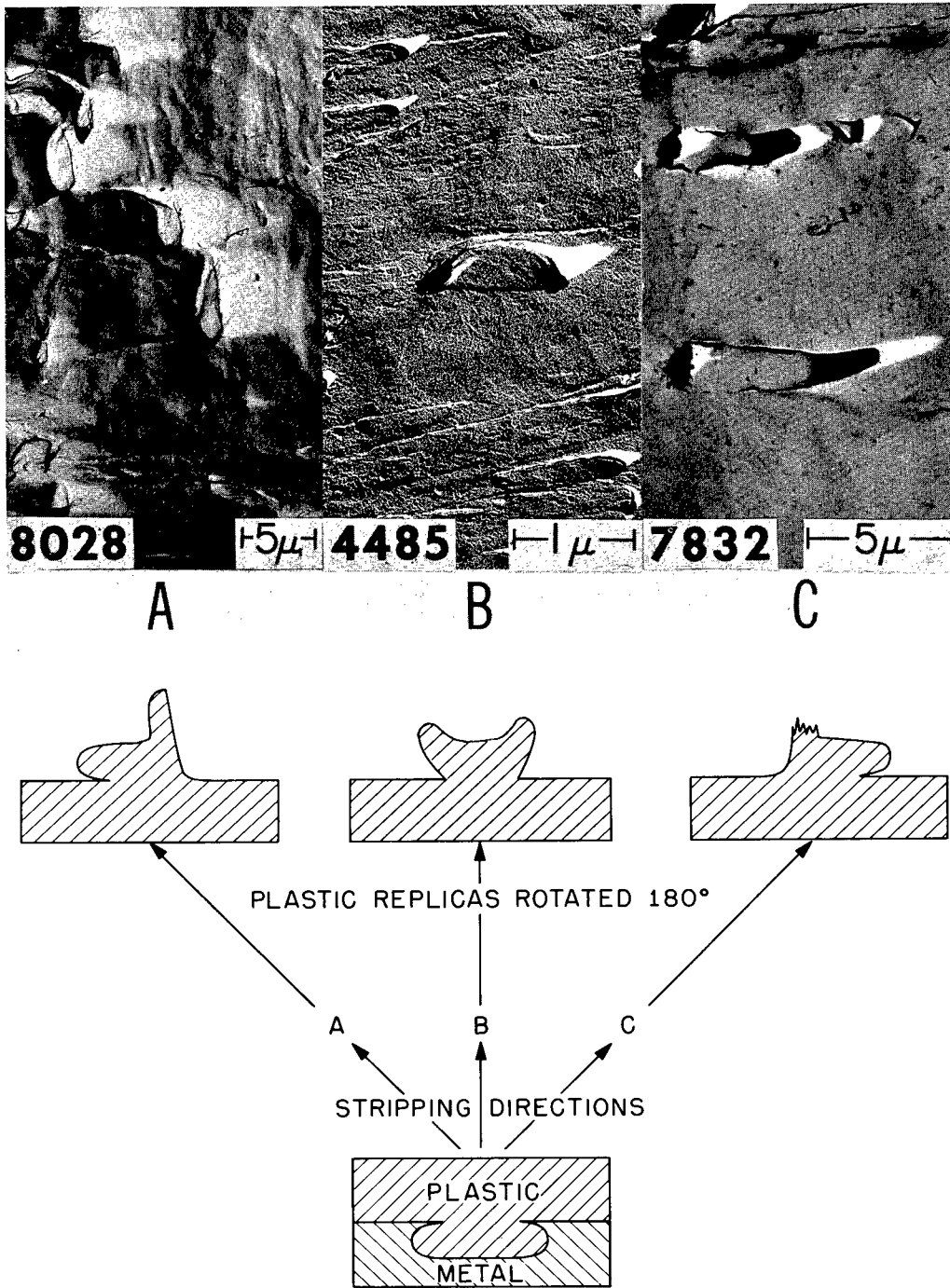


Fig. 30 — Examples and sketches of how two-stage (plastic-carbon) replicas of partially exposed voids on the fracture surface imperfectly reproduced the fracture surface, in contrast to the direct carbon replicas of Fig. 29. (Original magnifications: (A) 3000X, (B) 24,000X, and (C) 6000X.)



Fig. 31 - A further illustration of the superiority of a direct replication process. Tongues (arrows) are reproduced by the direct carbon process (top) but are not faithfully reproduced by the two-stage (cellulose acetate-carbon) process (bottom). (Original magnifications, 18,000X at the top and 15,000X at the bottom.)

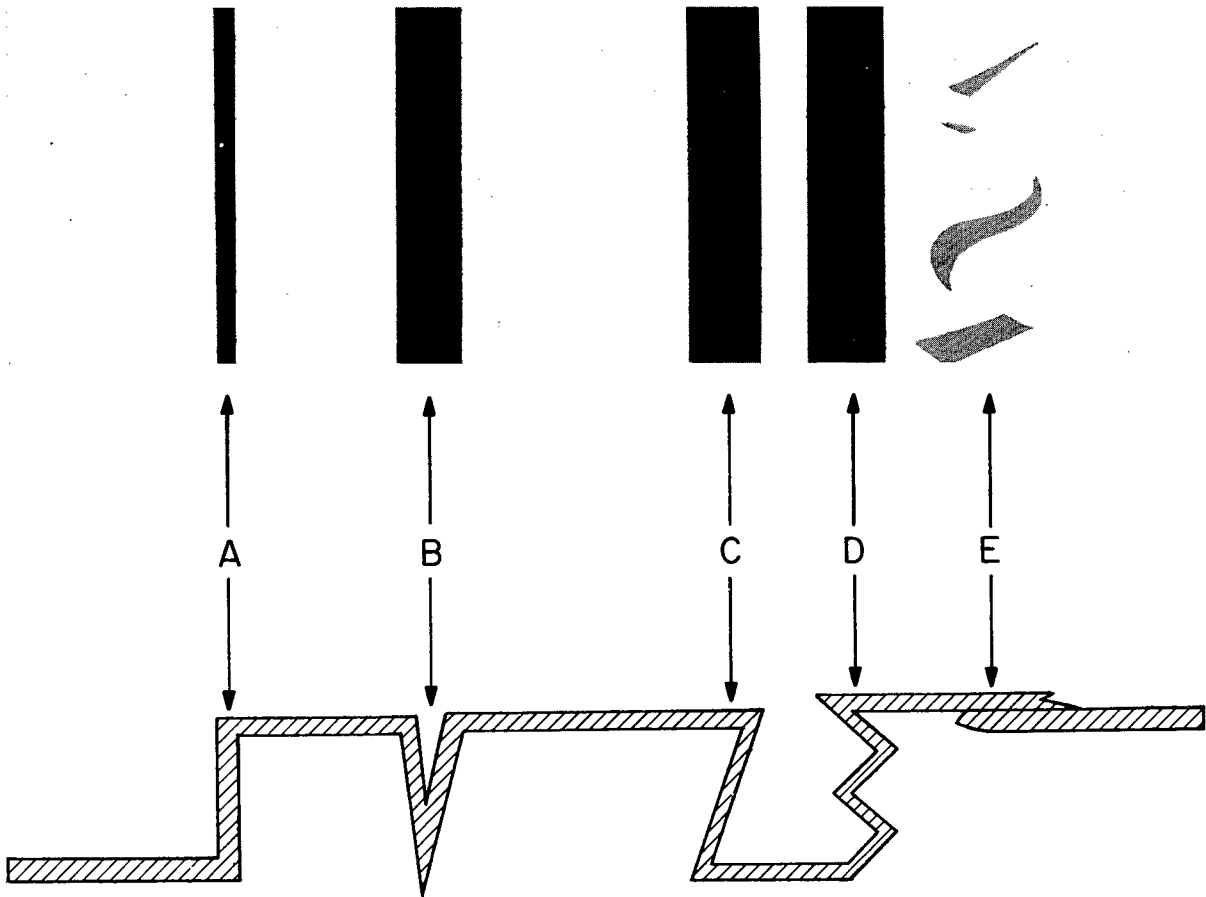


Fig. 32 – Illustrations of some of the features that give rise to opaque regions in replicas and an illustration of a tear in a replica

OTHER FACTORS OF INTERPRETATION

Stereo Viewing

Examination of replicas by stereo viewing provides a means of immediately seeing elevations—one does not have to figure out which features are depressions and which are hills from analyses of shadows each time he interprets a feature. Furthermore it makes direct quantitative measurements of heights, independent of shadows, possible.

Figure 33 is a stereo pair of a dimpled rupture surface with what appears as only a ragged dark band to the left in monoscopic viewing. Stereo viewing (see Appendix A) shows this dark band to be an overhanging cliff, apparently shaped the same as the original fracture surface, whereas

monoscopic viewing can only afford a guess at this. Without stereo viewing one often cannot say whether such a region is a collapsed portion of the replica or not. As shown in Fig. 32, any number of structures can give opaque regions. Only stereo viewing can permit many analyses such as these. Of course, if a feature is entirely opaque, even stereo viewing cannot divulge its internal shape. But it can permit the establishment of elevations of the perimeter of the opaque feature.

Depth Measurements

Depth measurements may be made from stereo pairs by measuring parallax differences in the two stereo pictures. Parallax is the distance between a specific point in one fractograph and

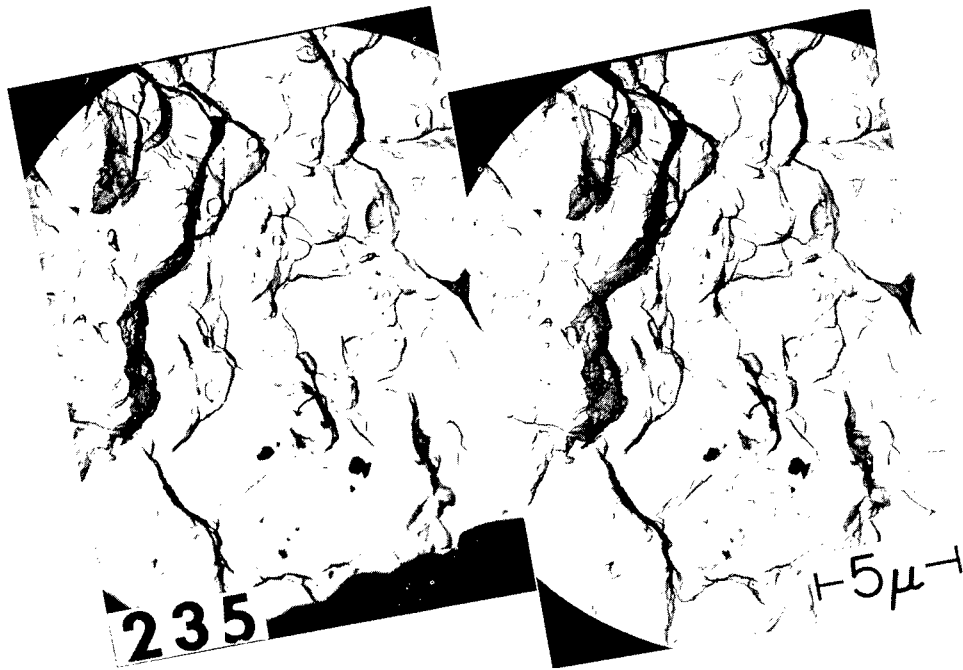


Fig. 33 – Stereo pair which illustrates the usefulness of stereo viewing in determining the shapes of such features as the overhanging cliff facing left that forms the dark band. This is a two-stage (cellulose acetate-carbon) replica of dimples in AISI 410 stainless steel, broken at room temperature. (The circular feature at the center is extraneous and was added for practice in unaided stereo viewing as explained in Appendix A.) (Original magnification, 4000X.)

the same point in the other fractograph when the two are side by side for stereo viewing. This distance is determined in part by the angle of tilt between the two orientations of the replica in the microscope with respect to the electron beam when the two fractographs were made. Points of different heights in the replica will have different distances between them from one fractograph to the other, with the highest point having the least distance, since the two views tilt toward each other.

Depths can be determined with the formula due to Edwards (12)

$$d = \frac{l_2 h_1 - h_2 l_1}{\sqrt{l_2^2 + h_2^2}} \quad (1)$$

using the dimensions shown in Fig. 34. The l 's in Eq. (1) are obtained from linear measurements on the surfaces of the fractographs (converted

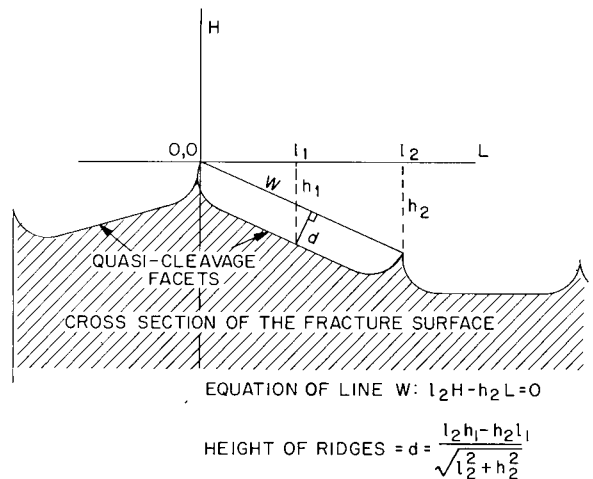


Fig. 34 – Nomenclature and method of depth measurements from stereo fractographs

to absolute lengths by dividing by the magnification) and the h 's are obtained from the following equation, also due to Edwards (12):

$$h = \frac{\Delta\rho}{2M \sin \frac{\theta}{2}} \quad (2)$$

where $\Delta\rho$ is the parallax difference, M is the total magnification, and θ is the angle of tilt between the two orientations of the replica when the two fractographs were made. The difference between the two parallaxes of two points, by Eq. (2), gives the difference in heights of the two points. In the case of Fig. 34, one point is used to fix a coordinate system, and the heights of two other points are determined relative to it.

Before making measurements such as these one should obtain a parallax bar with an accuracy of linear measurement of about 0.01 mm, and study the literature on measurements from stereo pictures (e.g., Ref. 13). One should also be forewarned that a great deal of time and effort is required for this work.

On flat surfaces one can, of course, calculate heights from a knowledge of the angle between the local substrate and the depositing vapor and a measurement of shadow length (1). If one does not know this angle, he may make two evaporations from two different directions, and from the difference in shadow lengths calculate the substrate angle (Ref. 1, page 332). Another technique is to place objects of known height on the replica, and let them cast shadows (10). Similar-triangle considerations can then permit the calculation of the heights of unknown features on the same flat surface. However, most fracture surfaces do not have large enough flat surfaces on them to permit these techniques on much of the replica.

Carbon Shadowing

Carbon, silicon monoxide, or some other chemically stable material is deposited or caused to form on the specimen or primary replica surface in the preparation of replicas to give the replica a continuous body. Most replicas are prepared by a metal-shadowing and "carbon-backing" technique.

Although the deposition of carbon is not thought of as a shadowing process, shadows are deposited. Figure 35 shows a polystyrene sphere which casts two shadows. Shadow A was cast during deposition of the metal and shadow

B was cast during the deposition of carbon. Shadow B would not have been cast if the replica had been rotated during the carbon evaporation. However, replica features such as shown in Figs. 36, 37, and 38 cannot help but cast some carbon shadows. The overhanging feature shown in Fig. 36a would cast a shadow whether it was rotated during carbon deposition or not. The same is true for the deep valleys shown in Fig. 37; not much depositing material can get down into the valleys. Figure 38 shows such a surface, with examples of valleys between hills shown between the arrows. The hills are, of course, pits in the metal surface.

When two evaporations are used to form the replica, and two shadows are cast as in Fig. 35, the heavier shadow normally would be that thrown by the metal. It is useful to use the direction of the metal shadows to denote, for example, the macroscopic crack propagation direction. However, on most fracture surface replicas, a sizeable proportion of the replica will not be exposed to the evaporated metal. When such regions are exposed to the depositing carbon, distinct carbon shadows are cast if the the replica is not rotated. Thus when one sees a single shadow of a feature which was not rotated during the deposition of either the metal or carbon, he does not have a foolproof way of knowing he is seeing the shadow caused by the metal and not the shadow caused by the carbon. Instead he has lost the ability to correlate the local shadow direction with macroscopic crack propagation direction. This is one of the reasons for rotating the substrate during the deposition of carbon. (The other reason is that it gives a more uniform—and thus perhaps stronger—layer of carbon.)

Orienting Stereo Pairs

The study of stereo fractographs is helpful in the interpretation of fracture mechanisms. One of the useful features of studying stereo pictures is that the relative elevations can be made to reverse by either interchanging the two pictures or by rotating each 180° under the viewer—hills become holes and *vice versa*. (The effect of reversal of the hills and holes can be seen by looking at stereo pairs in this report by the usual technique and then by a reversed

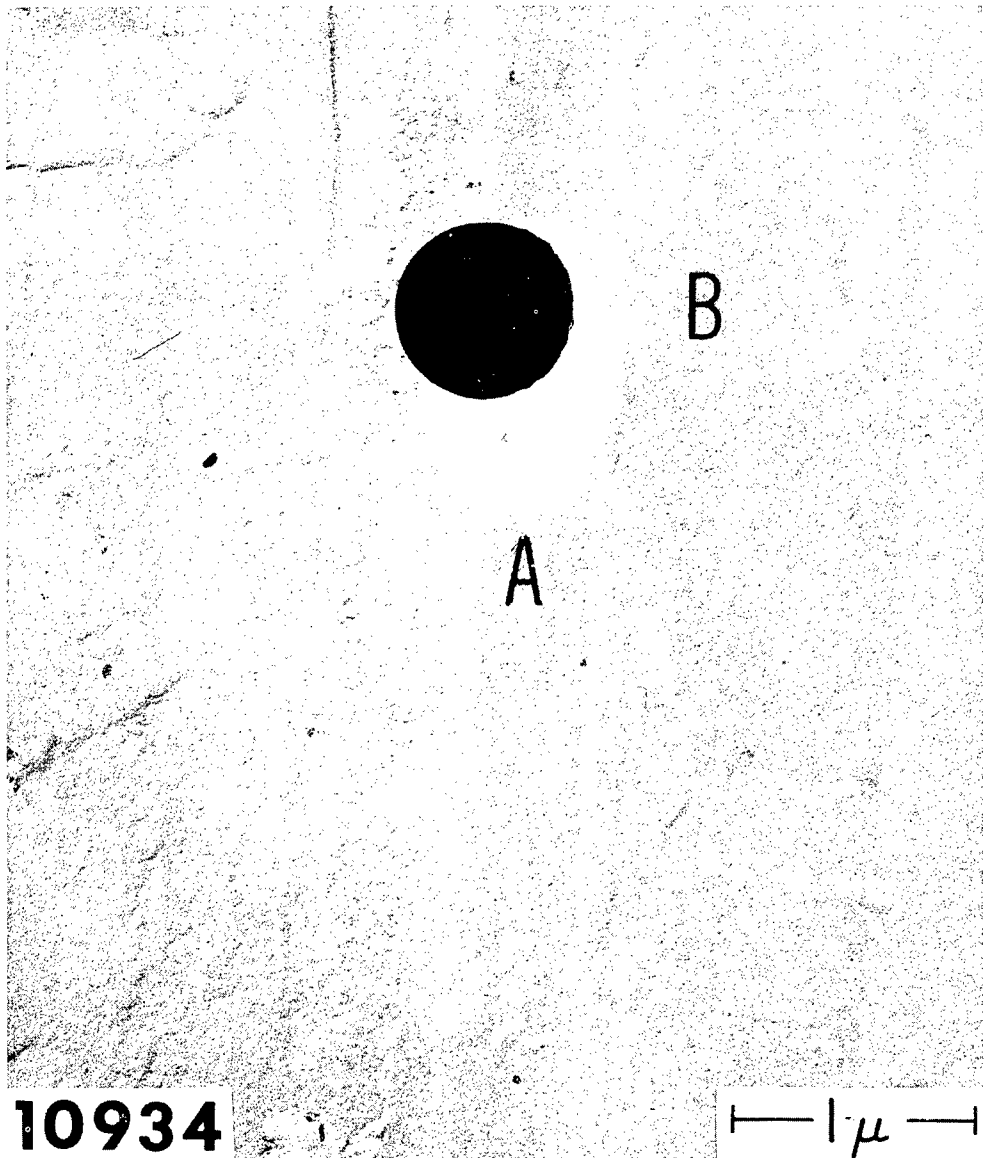


Fig. 35 — Comparison of palladium (A) and carbon (B) shadows cast by a polystyrene latex sphere on a cellulose acetate replica of a scratched glass microscope slide. (Original magnification, 34,000X.)

technique wherein the right-hand fractograph is viewed by the left eye and the left-hand fractograph is viewed by the right eye. To aid the eyes in merging the two images, one can first focus on a pencil point held midway to the stereo pair. This reversed technique is not recommended for routine viewing because it may be harder on the eyes.) Thus one may orient the pictures so that he is seeing the fracture

surface from outside the fractured piece or from inside the piece.

To decide which fractograph to place on the left and which to place on the right in order to see the fracture surface from outside the piece, when the shadowed replica was of cellulose acetate (negative replica), for example, one would *first look for distinct directional shadows*. Finding them, one may orient the pictures so

001
002
003
004
005
006
007
008
009
010
011
012
013

ROTARY CARBON DEPOSITION

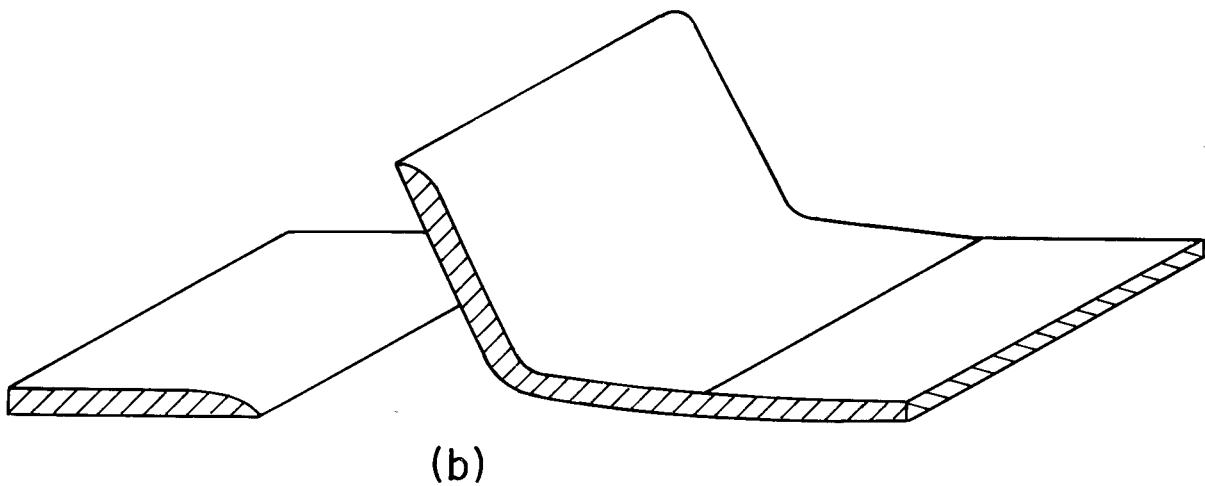
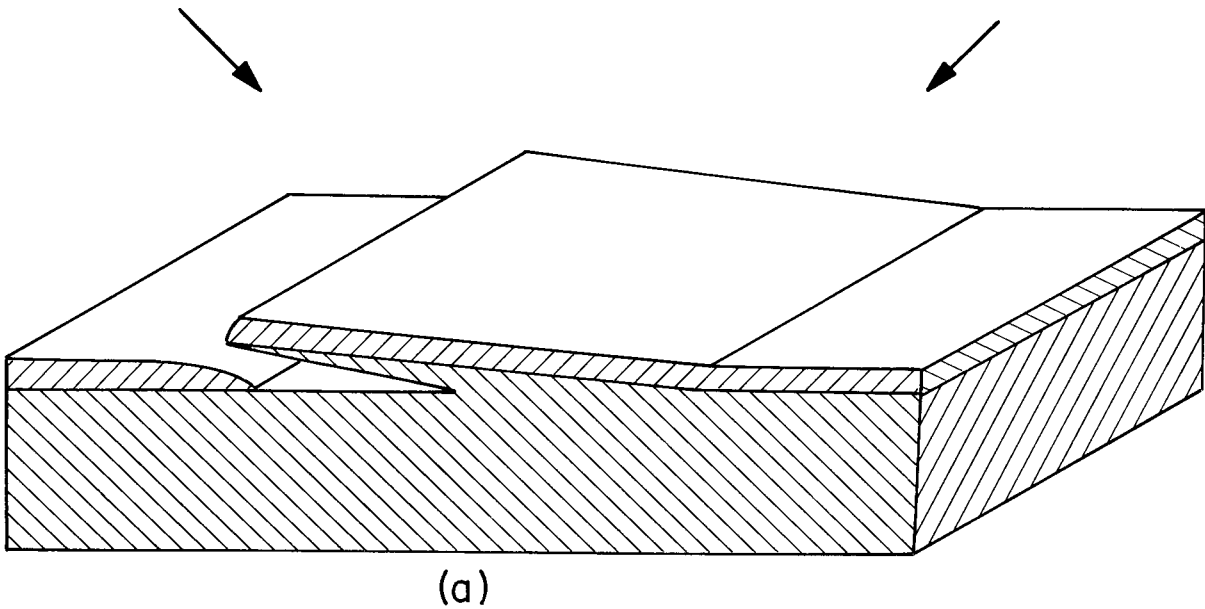
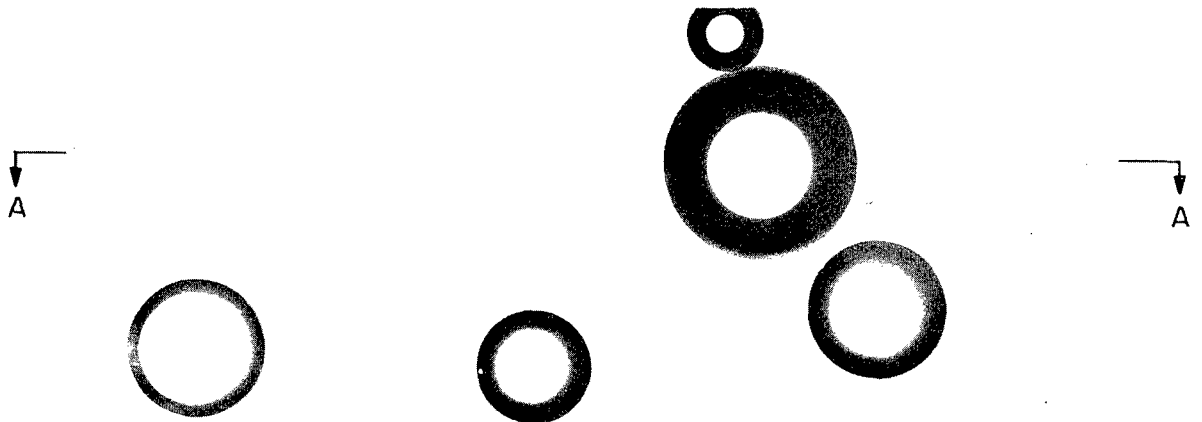


Fig. 36 - Illustration of how a nondirectional carbon shadow can be misinterpreted as a directional metal shadow. During replica washing or mounting on grids, features that cast such shadows sometimes change their orientations, as from (a) to (b).

that an object which casts a shadow outside itself appears as a depression or extends down away from the observer. Or, if a given feature contains its own shadow, this can be made to appear as

a hill by correct orientation of the fractographs. Frequently, however, one cannot find distinct shadows, as in Fig. 26 for example. In such cases, one can often determine the proper orientation



CARBON DEPOSITED AT 45° WHILE SUBSTRATE IS ROTATED

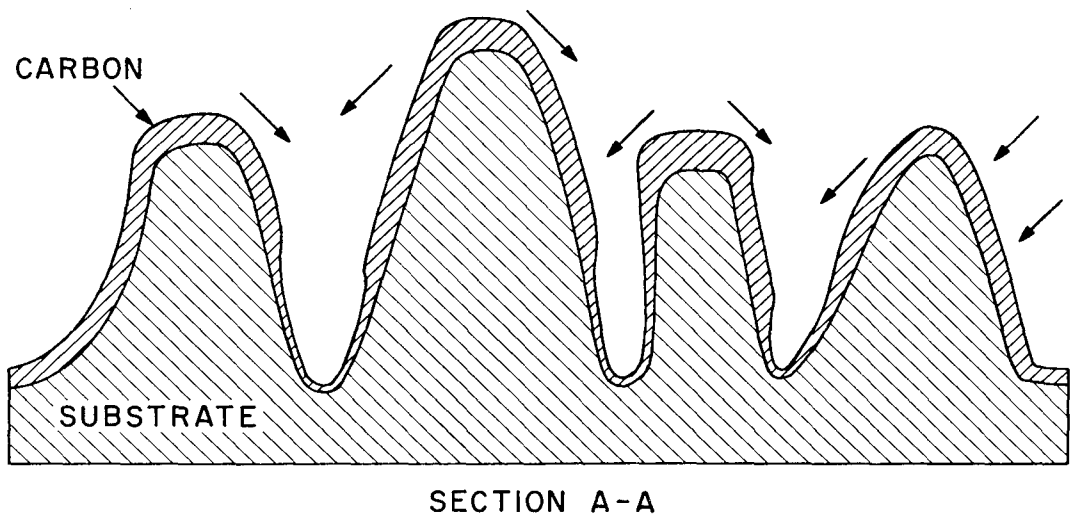


Fig. 37 - Another illustration of nondirectional carbon shadowing, showing how carbon cannot deposit as heavily in the valleys as it can on the hills

of the stereo pictures by *finding features of known shape*. The dimples in Fig. 26 are known to be concave on the fracture surface, so one just makes them look that way in order to know that he is viewing the fracture surface from outside the piece. When neither distinct directional shadows nor known features are available, one can sometimes orient the stereo pairs by *observing nondirectional carbon shadows*. There are usually some features on the

surface during evaporation that cast some kind of shadow. Figure 38 is a good example of this. In order to know that the observer was seeing the fracture surface from outside the piece, in this case it was necessary to orient the stereo pair so that the most dense regions appeared as the bottoms of holes or valleys. (The bottoms of the valleys in the plastic replica were thin, and thus these thin regions were the tops of hills on the fracture surface.)

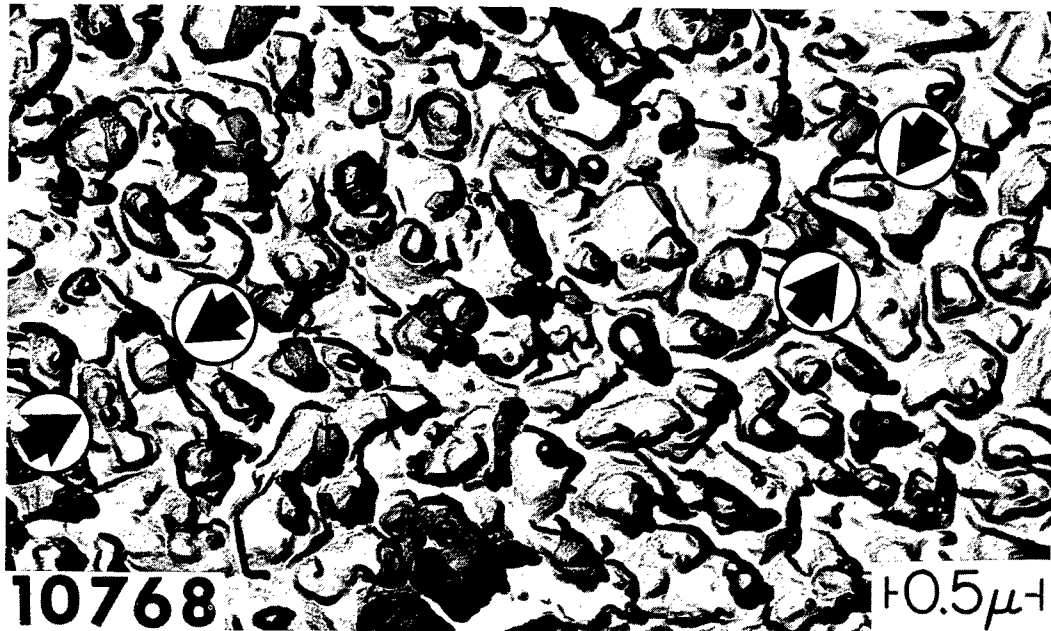


Fig. 38 — Example of a surface similar to that sketched in Fig. 37. Pairs of hills with a valley between each pair, are shown between arrows. This is a two-stage (cellulose acetate-carbon) replica of type 304 stainless steel, stress-corrosion cracked in boiling $MgCl_2$. (Original magnification, 45,000X.)

If there are no distinct shadows, no known features, and no nondirectional carbon shadows in the particular fractographs under study, the only thing which will permit proper orientation of stereo fractographs is meticulous record keeping of the orientation of the replica from start to finish. Happily, this is seldom necessary.

The difficulty of proper stereo pair orientation increases with increasing magnification, because when less of the replica is seen in one stereo pair, one has a poorer sampling of the replica, and often the degree of magnification is reached where only a few features are seen which cast shadows. As shown in Fig. 36, it is potentially dangerous to use only a single shadow to determine orientation. In this sketch a feature which casts a distinct carbon shadow is seen to change its orientation during some stage of replica preparation (after shadow casting), and when seen in stereo, appears to have been erect during metal shadowing, casting a directional shadow. The real metal shadow would probably be in some other direction, had one been cast. Another example of this danger is shown in Fig. 39. Here the projection on the left (A) casts a shadow

onto another projection (B) to its right. The top sketch shows that only one opaque region may be seen on the fractograph, and stereo viewing may not enable one to sense the relative height of the opaque region with respect to the height of the shadow. Under such circumstances one might erroneously believe that the replica to the right of the opaque region was a depression at the time of shadowing since it appears to contain its own shadow. *One must make certain, therefore, in determining orientation of stereo pairs, that the shadows he is using as a guide were in fact cast by the objects under consideration and that the shadows are in fact the shadows that he is looking for* (usually the metal shadow as contrasted to a carbon shadow). These difficulties are seldom encountered when several shadows are seen in the fractographs.

Precision Matching

The option of orientation of stereo pairs is useful in precision matching studies. When two mating metal fracture surfaces are seen side-by-side with the unaided eye, one is "the mirror

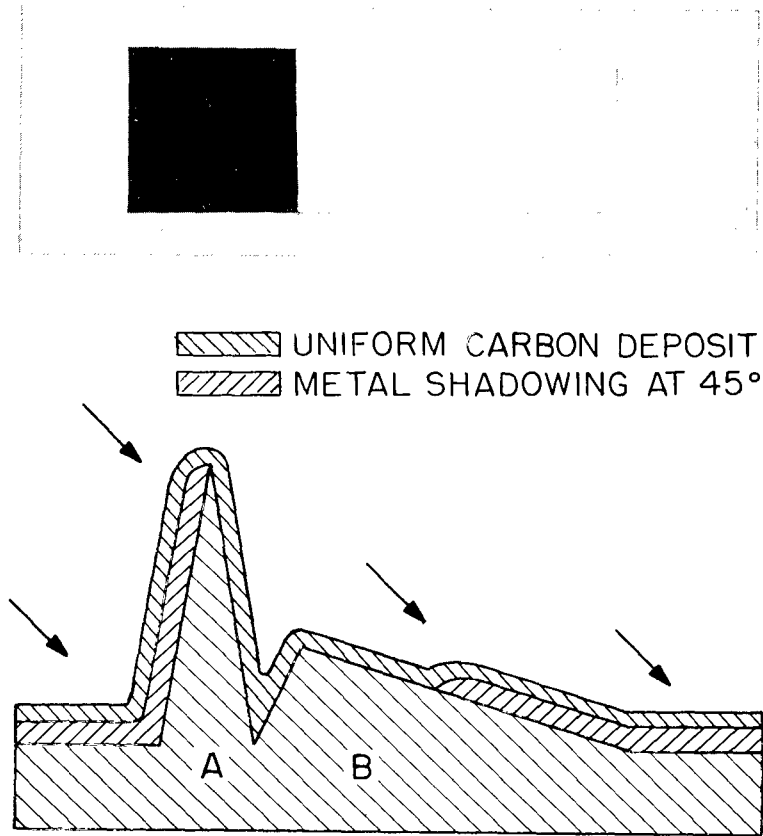


Fig. 39 - An example of how observations of a single shadow can lead to misinterpretation

image" of the other. A detail on the lower left of one will be matched by a detail on the lower right of the other, for example. In precision matching studies, interpretation is facilitated by printing the pictures so that this "mirror image" effect is changed so that a detail in the lower left of one fractograph is matched by the mating detail in the lower left of the other. This is often accomplished by printing one picture with the negative emulsion up and the other with the emulsion down. When the stereo pictures are printed in this manner, one can imagine that he is seeing one surface from outside the piece and the other surface from inside. This concept can be used in the orientation of the two sets of stereo pictures under the viewer in such a manner that the observer sees both surfaces simultaneously. He may then proceed to make quick observations as to whether or not a projection on the surface fits into a depression on

the other, and so on. An example of such an exercise is shown in Fig. 40, which is printed for unaided visual stereo viewing.* These are direct carbon replicas, so that when a feature contains its own shadow, the stereo pair should be oriented so that this feature is a hole if one wishes to see the fracture surface from outside the piece. The top stereo pair is oriented this way. The bottom pair is oriented so that the observer sees this matching fracture surface from inside this matching piece. The inverted V extending across the two top fractographs is seen to be the top of a sharp ridge in stereo, which then is a ridge on the real fracture surface. The matching feature on the bottom pair is seen as the bottom of a sharp groove, and since we are seeing this surface from inside the matching piece the line

*Figure 40 is reprinted in Appendix B to permit it to be removed if one wishes to use a viewer.



Fig. 40 - Stereo pairs of matching fracture surfaces in 7075-T6 aluminum alloy, showing a large stretched region at the bottom of each fractograph and tear dimples at the top. These are palladium-shadowed direct carbon replicas of the matching surfaces. (Original magnification, 4000X.)

is again the top of a ridge on the real fracture surface of the matching piece. The interpretation therefore is that this particular region of the metal piece broke by tearing (14), and a tear ridge (15) was formed on both fracture surfaces.

Tailoring of Replicas

Interpretation is aided significantly by tailoring the replication technique and procedure to

the surface to be observed. One must have some good idea of what he wants to see in the microscope before he makes his replica. If, for example, he wants to study very fine fatigue striations, the shadowing metal should be evaporated perpendicular to the striations rather than parallel to them. He then would have the best chance of seeing them if he evaporated in the direction of macroscopic fatigue crack propagation (since the striations represent successive

positions of the crack front). Striations in some instances cannot be seen unless they are thus properly shadowed.

One must be extremely careful when he attempts to precisely match two mating surfaces. Not only does he want to be able to complete his study, but he wants to have clean, sharp pictures for illustrating his findings when he publishes his results. In these cases, particular areas on both surfaces must be shadowed at the same angle and the same density – otherwise one picture will appear crisp and the other will appear washed-out.

The prior knowledge of the size of things that are to be observed is also useful in making replicas. Features to be photographed at or below 1000X should have much more shadow and carbon than those which are to be photographed at 30,000X. It is certain that one cannot get the best possible pictures at both magnifications from the same replica. If a replica is made very thin so that the 0.01μ features are shown in good fidelity, then the 10 or 20μ features are quite likely to collapse or rip, and they will not be dense enough, or have enough contrast, to make a good picture.

To decide upon the thickness of the replica, then, one needs to consider two factors. First, the thickness of the film should be small in relation to the objects to be observed. Secondly, the film should be as thick as is permissible to give it as much strength as possible. This is offered only as a qualitative rule—no actual measurements of replica thicknesses have been made with relation to fidelity of specific sizes of objects and strengths of the replicas.

The need to make replicas thin in relation to the size of replica features to be studied is real and important, particularly at high magnifications (30,000X and above). A 1000\AA -thick carbon film is 0.1μ thick, and this is quite an appreciable slab when one considers that at 30,000X this 0.1μ becomes 3 mm or $1/8$ inch. Likewise, of course, a 100\AA -thick replica (which is a reasonably thin replica) is thick enough so that details on the original fracture surface that appear on a 30,000X final print as 0.3 mm in size, has a coating of an additional 0.3 mm. This may well mean that it would be three times as big on the fractograph as it really was on the original fracture. Thus it is the interpretation of small

features on high magnification fractographs which require careful consideration of replica-techniques and replica thicknesses.

In the earlier discussion of the shadow thickness and in the sketches of shadowed replicas, this relation between feature size and replica thickness was not mentioned. But if one considers Figs. 8, 9, 16, 37, and 41, he sees that during replica formation, hills become larger, while holes remain the same size but tend to fill up. With normal fractographic replica techniques, where one uses 75 or 100 mesh grids, the replica is thick enough (several hundred angstroms) so that this thickness must be taken into account during interpretation. Figure 41 illustrates the kind of potential trouble which one might seek to avoid in high magnification examination of fracture surface replicas. In this case a thick shadow on one side of a rounded projection, combined with high contrast photography, might cause an unwary observer to think that an actual surface of rounded pits was formed by shear rupture (14). In failure analysis work, this could be seriously misleading.

REPLICA FIDELITY

The degree to which the final printed fractograph represents the original fracture surface is affected by many things. Identification of artifact structures is usually accomplished by the process of making and studying many replicas of many fracture surfaces (where the material and test conditions are pedigreed) and thereby developing a knowledge of what the fracture surfaces ought to look like. The real test of fidelity is to take successive replicas from the same fracture surface and, after precision matching is accomplished, comparing the fine detail in the various replicas. This is time consuming and is seldom done.

One major limitation of replica fidelity arises from the fragility of the replica. It is thin with respect to the diameter of the grid, and each micron-sized portion of the replica is about 50 to 100 times as wide as it is thick. These thin composite sheets of metal and carbon obey the same laws as any other sheet of stiff material. They can be easily bent around one axis, as shown in Fig. 21, but will tear or fold if forces tend to bend them simultaneously around two axes.

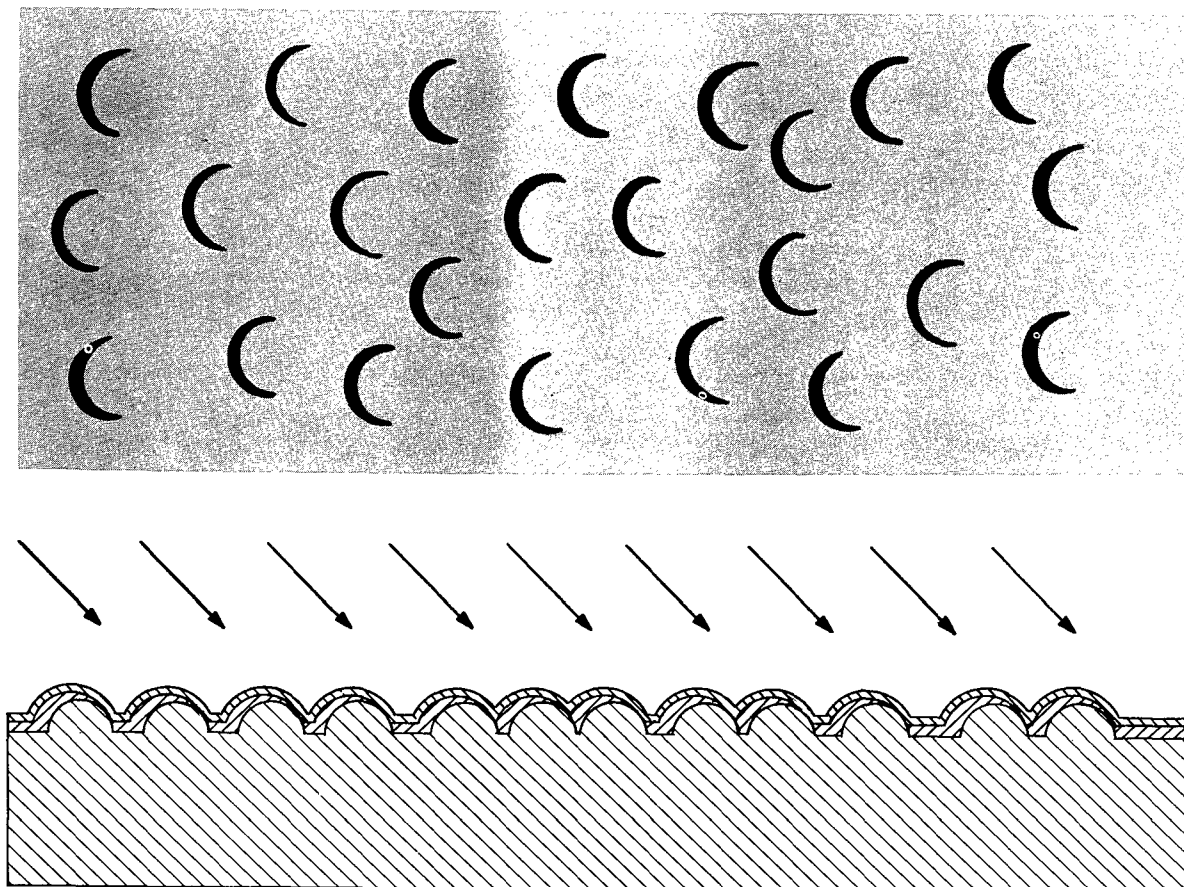


Fig. 41 — An example of how the thickness of deposited metal, combined with high magnifications and high-contrast photography, can lead to misinterpretation

They cannot be stretched in a direction which lies in their plane, but will tear. However, if several neighboring portions of the replica form an undulating or accordion-bellows shape, the composite may stretch without tearing by slightly bending each of its component parts.

The shape of each individual portion (*e.g.*, facet) of the replica is frequently maintained by the strengthening nature of adjacent parts. Each of the thin, flat intergranular facets in Figs. 10 and 11, for example, holds its shape because the neighboring facets act as stabilizers. This is similar to the stability of triangles and tetrahedrons. If one sees a place on a replica, however, where a facet is torn or deformed, he can be fairly certain that this distortion is somehow transmitted to some of the immediate neighbors.

In considering the relative thinness of replicas, one must realize that the forces of cellulose acetate expansion, and often even worse, the forces of liquid surface tension during replica drying are quite sufficient to cause severe local damage to the replica. Portions of the replica tear or fold, or collapse, or rotate, or rumple, and the replica—as seen in the microscope—never completely represents the original fracture surface. Consideration of each detail, and the strengthening or weakening capabilities of its immediate neighbors, is necessary in determining replica fidelity.

SUMMARY AND CONCLUDING REMARKS

This report was prepared to aid the relative newcomer to the field of electron fractography in the interpretation of fractographs.

Accurate interpretation depends upon an understanding of the various effects of microscope and replica variables upon the photographic density of specific portions of each fractograph. Photographic contrast decreases with increasing electron gun potential and lens aperture size. Electron density decreases and hence the photographic density of the printed fractograph increases with the amount of replica material penetrated by the electrons. This, in turn, increases with an increase of the local thickness of the replica, or a decrease in the angle between the local replica surface and the incident electron beam.

The thickness of the replica depends upon the vacuum in the bell jar during formation of the replica, the angle of the feature with respect to the depositing metal or carbon, and the distance between the feature and the source of the carbon or metal. Surfaces oriented at different angles to the depositing material thus have different densities, with flat facets having uniform densities throughout each facet and curved surfaces having gradually changing densities.

Features which were concave at the time of shadowing contain their own shadows and tend to remain the same size but to fill up with shadowing material, while features which were convex cast external shadows and tend to grow larger.

Interpretation is aided significantly by the use of stereoscopic viewing. The viewer can immediately establish relative heights and shapes of features and with time and practice can make measurements of heights by using stereo viewing. Precision matching studies of mating fracture surfaces is a useful technique in proving fracture mechanisms.

Replicas should be made thin for high magnification studies and thick for low magnification studies. Replica fidelity is a function of the choice of replication technique and the shape of both the features under study and immediately adjacent portions of the replicas.

This report can be only an aid to the newcomer, since nothing can adequately replace individual carefulness and experience. Every portion of every fracture surface is to some extent unique, since local fracture mechanisms are largely dependent upon local microstructural con-

stituent properties and orientations and how these react to local stresses and environments. One thus finds that fracture surfaces usually contain several species of features. Thus the analyst must use additional time and patience in *properly sampling* various portions of each replica and must make replicas of representative regions of each specimen before he can characterize fracture surfaces in any one material broken under any one set of conditions. A few observations from one replica from one specimen are insufficient for most applications of fractography. In addition it is recommended that a sizeable portion of an hour be used in interpreting each fractograph that shows new features or new combinations of features, *i.e.*, most fractographs.

REFERENCES

1. Hall, C.E., "Introduction to Electron Microscopy," New York:McGraw-Hill (1953)
2. Kay, D., editor, "Techniques for Electron Microscopy," Springfield, Illinois, Charles C. Thomas, publisher, (1961)
3. Haine, M.E., "The Electron Microscope—The Present State of the Art," New York:Interscience (1961)
4. Thomas, G., "Transmission Electron Microscopy of Metals," New York:Wiley (1962)
5. Dahlberg, E.P., "An Electron Microscope Study of Crack Surfaces in a Tungsten Rocket Nozzle Insert," NRL Memorandum Report 1217, September 1961
6. Meyn, D.A., "A Study of the Crystallographic Orientation of Cleavage Facets Produced by Stress-Corrosion Cracking of Ti-7Al-2Nb-1Ta," paper to be presented at the 1965 Fall Meeting of the AIME
7. Meyn, D.A., Beachem, C.D., and Lupton, T.C., "Observations Made at the Root of a Notch in Iron Fatigued in Bending," NRL Memorandum Report 1614, May 1965
8. Dahlberg, E.P., "Characteristics of Twinning on Fracture Surfaces of Single and Polycrystalline Tungsten," *Fifth International Congress for Electron Microscopy*, Vol. 1, p. J-5, Academic Press, New York (1962)
9. Beachem, C.D., and Dahlberg, E.P., "Fractography. Part XV. Some Artifacts Possible with the Two-Stage Plastic Carbon Replication Technique," NRL Memorandum Report 1457, September 1963
10. Phillips, A., Kerlins, V., and Whiteson, B.V., "Electron Fractography Handbook," Technical Report ML-TDR-64-416, Air Force Materials Laboratory, Research and Technology Division, Air Force Systems Command, Wright-Patterson Air Force Base, Ohio, 31 January 1965
11. Beachem, C.D., and Meyn, D.A., "Illustrated Glossary of Fractographic Terms, Section 2, Glide Plane Decohesion, Serpentine Glide, Ripples, Stretching, Microvoid Coalescence," NRL Memorandum Report 1547, June 1964
12. Edwards, A.J., "Gases in Steel (Depth Measurements on Fracture Surfaces)," Report of NRL Progress, November 1963

13. Smith, H.T.U., *Aerial Photographs and Their Applications*, Appleton-Century-Crofts, Inc., New York (1943)
14. Beachem, C.D., "An Electron Fractographic Study of the Influence of Plastic Strain Conditions Upon Ductile Rupture Processes in Metals," *Transactions ASM*, Vol. 56, 318 (1963)
15. Dahlberg, E.P., "Fatigue-Crack Propagation in High-Strength 4340 Steel in Humid Air," *Transactions ASM*, Vol. 58, 46 (1965)

001
002
003
004
005
006
007
008
009
010
011
012
013
014
015
016
017
018
019
020
021
022
023
024
025
026
027
028
029
030
031
032
033
034
035
036
037
038
039
040
041
042
043
044
045
046
047
048
049
050
051
052
053
054
055
056
057
058
059
060
061
062
063
064
065
066
067
068
069
070
071
072
073
074
075
076
077
078
079
080
081
082
083
084
085
086
087
088
089
090
091
092
093
094
095
096
097
098
099
100

010
011
012
013
014
015
016
017
018
019
020
021
022
023
024
025
026
027
028
029
030
031
032
033
034
035
036
037
038
039
040
041
042
043
044
045
046
047
048
049
050
051
052
053
054
055
056
057
058
059
060
061
062
063
064
065
066
067
068
069
070
071
072
073
074
075
076
077
078
079
080
081
082
083
084
085
086
087
088
089
090
091
092
093
094
095
096
097
098
099
100

Appendix A

FIGURE FOR PRACTICING UNAIDED STEREO VIEWING

Figure A1 is a repetition of Fig. 33 which is reprinted here to permit the following experiment. A number of people have developed the capability of seeing stereo by merely holding the stereo pair up in front of them and looking at it. If the reader has not developed this capability, he may punch or cut holes at the indicated places near the center of each of the two fractographs in Fig. A1 and, while holding the page at a distance of about arm's length, look at a point on the horizon (or a few hundred feet away) through the holes. This should be done with the left eye looking through the hole in the left-hand fractograph and the right eye looking through the hole in the right-hand fractograph. When the page is properly oriented the two holes should be exactly merged together at the center of the

page. The page should be rotated back and forth to "zero in" on the exact merger of the holes. After staring at the point on the horizon for several minutes and then relaxing the eyes while switching awareness to a detail of the replica, one should realize the sense of depth in the stereo pair. The page may again have to be rotated back and forth a bit to achieve the sharpest clarity. With a little practice, one should be able to merge the images without looking through the holes at the horizon. He should then be able to see depth in the other stereo pairs in this report without special equipment by selecting a prominent feature of the replica, and (with the left eye looking at the feature in the left fractograph and the right eye looking at the feature in the right fractograph) making the two images merge.

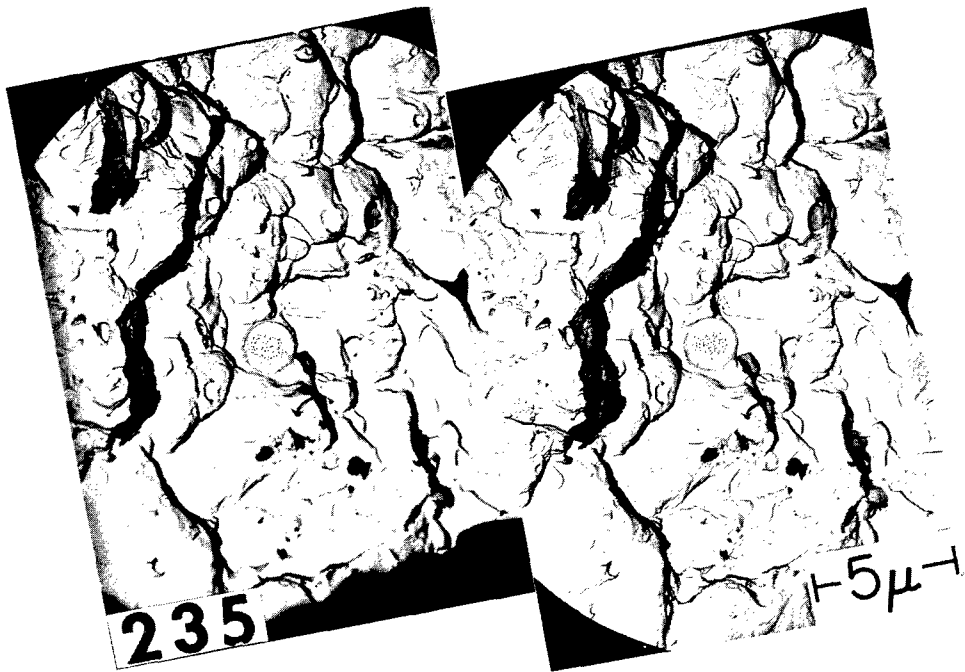


Fig. A1 - Reprint of Fig. 33

112
113
114
115
116
117
118
119
120

Appendix B

REPRINT OF FIG. 40 TO PERMIT REMOVAL

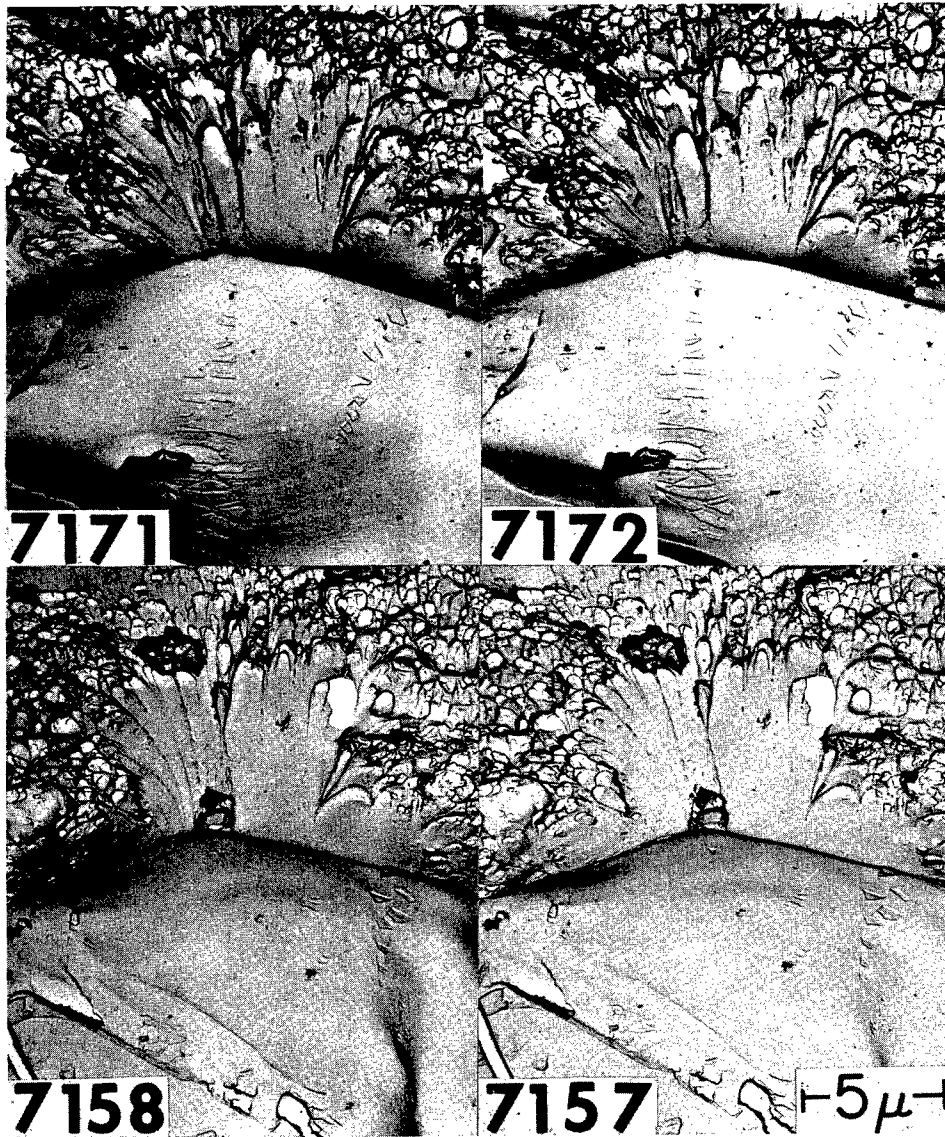


Fig. B1 - Reprint of Fig. 40

DOCUMENT CONTROL DATA - R&D

(Security classification of title, body of abstract and indexing annotation must be entered when the overall report is classified)

1. ORIGINATING ACTIVITY <i>(Corporate author)</i> U.S. Naval Research Laboratory Washington, D.C. 20390		2 a. REPORT SECURITY CLASSIFICATION UNCLASSIFIED	
		2 b. GROUP	
3. REPORT TITLE THE INTERPRETATION OF ELECTRON MICROSCOPE FRACTOGRAPHS			
4. DESCRIPTIVE NOTES <i>(Type of report and inclusive dates)</i> Interim report on the problem; final report on material to aid newcomers in electron fractography.			
5. AUTHOR(S) <i>(Last name, first name, initial)</i> Beachem, C.D.			
6. REPORT DATE January 21, 1966		7 a. TOTAL NO. OF PAGES 54	7 b. NO. OF REFS 15
8 a. CONTRACT OR GRANT NO. M01-08		9 a. ORIGINATOR'S REPORT NUMBER(S) NRL Report 6360	
b. PROJECT NO. RRMA 02-061/652-1/R007-01-01			
c. RR 007-01-46-5406		9 b. OTHER REPORT NO(S) <i>(Any other numbers that may be assigned this report)</i>	
d.			
10. AVAILABILITY/LIMITATION NOTICES Distribution of this report is unlimited.			
11. SUPPLEMENTARY NOTES		12. SPONSORING MILITARY ACTIVITY Department of the Navy (Office of Naval Research and Bureau of Weapons)	
13. ABSTRACT This report was prepared to aid the relative newcomer to electron fractography in the interpretation of fractographs. Accurate interpretation depends on understanding the effects of electron-microscope and replica variables on photographic densities in the fractographs. Briefly, some of these effects are as follows: Contrast decreases with increasing electron gun potential and lens aperture size. Electron density decreases and hence photographic density in the printed fractograph increases with the amount of replica material penetrated by the electrons. This, in turn, increases with an increase in the local thickness of the replica or with a decrease in the angle between the local replica surface and the incident electron beam. The thickness of the replica depends on the vacuum in the bell jar during formation of the replica, the angle of the local feature with respect to the depositing metal or carbon, and the distance between the feature and the source of the carbon or metal. During shadowing, convex features cast external shadows and tend to grow larger, while concave features contain their shadows and tend to remain the same size but to fill up with shadowing material. Interpretation is aided by stereoscopic viewing and by precision matching of mating fracture surfaces. Replica fidelity is a function of the choice of replication technique, with the direct carbon process generally being superior, and of the shape of both the features under study and immediately adjacent portions of the replicas. This report can be only an aid to the newcomer, since nothing can adequately replace individual carefulness and experience. A fracture surface usually contains several species of features, and a few observations from one replica from one specimen are insufficient for most applications of fractography.			

012
013
014
015
016
017
018
019
020
021
022
023
024
025

14. KEY WORDS	LINK A		LINK B		LINK C	
	ROLE	WT	ROLE	WT	ROLE	WT
Fracture (Mechanics) Metallurgy Electron Microscopes Stereoscopes Fractography Interpretation Replicas Fracture Surfaces Instructions for Newcomers						

INSTRUCTIONS

1. **ORIGINATING ACTIVITY:** Enter the name and address of the contractor, subcontractor, grantee, Department of Defense activity or other organization (*corporate author*) issuing the report.

2a. **REPORT SECURITY CLASSIFICATION:** Enter the overall security classification of the report. Indicate whether "Restricted Data" is included. Marking is to be in accordance with appropriate security regulations.

2b. **GROUP:** Automatic downgrading is specified in DoD Directive 5200.10 and Armed Forces Industrial Manual. Enter the group number. Also, when applicable, show that optional markings have been used for Group 3 and Group 4 as authorized.

3. **REPORT TITLE:** Enter the complete report title in all capital letters. Titles in all cases should be unclassified. If a meaningful title cannot be selected without classification, show title classification in all capitals in parenthesis immediately following the title.

4. **DESCRIPTIVE NOTES:** If appropriate, enter the type of report, e.g., interim, progress, summary, annual, or final. Give the inclusive dates when a specific reporting period is covered.

5. **AUTHOR(S):** Enter the name(s) of author(s) as shown on or in the report. Enter last name, first name, middle initial. If military, show rank and branch of service. The name of the principal author is an absolute minimum requirement.

6. **REPORT DATE:** Enter the date of the report as day, month, year, or month, year. If more than one date appears on the report, use date of publication.

7a. **TOTAL NUMBER OF PAGES:** The total page count should follow normal pagination procedures, i.e., enter the number of pages containing information.

7b. **NUMBER OF REFERENCES:** Enter the total number of references cited in the report.

8a. **CONTRACT OR GRANT NUMBER:** If appropriate, enter the applicable number of the contract or grant under which the report was written.

8b, 8c, & 8d. **PROJECT NUMBER:** Enter the appropriate military department identification, such as project number, subproject number, system numbers, task number, etc.

9a. **ORIGINATOR'S REPORT NUMBER(S):** Enter the official report number by which the document will be identified and controlled by the originating activity. This number must be unique to this report.

9b. **OTHER REPORT NUMBER(S):** If the report has been assigned any other report numbers (*either by the originator or by the sponsor*), also enter this number(s).

10. **AVAILABILITY/LIMITATION NOTICES:** Enter any limitations on further dissemination of the report, other than those imposed by security classification, using standard statements such as:

- (1) "Qualified requesters may obtain copies of this report from DDC."
- (2) "Foreign announcement and dissemination of this report by DDC is not authorized."
- (3) "U. S. Government agencies may obtain copies of this report directly from DDC. Other qualified DDC users shall request through _____."
- (4) "U. S. military agencies may obtain copies of this report directly from DDC. Other qualified users shall request through _____."
- (5) "All distribution of this report is controlled. Qualified DDC users shall request through _____."

If the report has been furnished to the Office of Technical Services, Department of Commerce, for sale to the public, indicate this fact and enter the price, if known.

11. **SUPPLEMENTARY NOTES:** Use for additional explanatory notes.

12. **SPONSORING MILITARY ACTIVITY:** Enter the name of the departmental project office or laboratory sponsoring (*paying for*) the research and development. Include address.

13. **ABSTRACT:** Enter an abstract giving a brief and factual summary of the document indicative of the report, even though it may also appear elsewhere in the body of the technical report. If additional space is required, a continuation sheet shall be attached.

It is highly desirable that the abstract of classified reports be unclassified. Each paragraph of the abstract shall end with an indication of the military security classification of the information in the paragraph, represented as (TS), (S), (C), or (U).

There is no limitation on the length of the abstract. However, the suggested length is from 150 to 225 words.

14. **KEY WORDS:** Key words are technically meaningful terms or short phrases that characterize a report and may be used as index entries for cataloging the report. Key words must be selected so that no security classification is required. Identifiers, such as equipment model designation, trade name, military project code name, geographic location, may be used as key words but will be followed by an indication of technical context. The assignment of links, roles, and weights is optional.